

**SIGNIFICANT CONTRASTS OF AEROSOL ACIDITY BETWEEN  
CHINA AND THE UNITED STATES**

A Dissertation  
Presented to  
The Academic Faculty

by

Bingqing Zhang

In Partial Fulfillment  
of the Requirements for the Degree  
Master of Science in the  
School of Civil and Environmental Engineering

Georgia Institute of Technology  
May 2021

**COPYRIGHT © 2021 BY BINGQING ZHANG**

**SIGNIFICANT CONTRASTS OF AEROSOL ACIDITY BETWEEN  
CHINA AND THE UNITED STATES**

Approved by:

Dr. Armistead Russell, Advisor  
School of Civil and Environmental Engineering  
*Georgia Institute of Technology*

Dr. James Mulholland  
School of Civil and Environmental Engineering  
*Georgia Institute of Technology*

Dr. Jennifer Kaiser  
School of Civil and Environmental Engineering  
*Georgia Institute of Technology*

Date Approved: April 14 2021

## TABLE OF CONTENTS

LIST OF TABLES	ii
LIST OF FIGURES	iii
SUMMARY	iv
CHAPTER 1. Introduction	1
CHAPTER 2. Data collection and study method	4
2.1 Observational data	4
2.2 Model configuration	8
2.3 Aerosol pH calculation	9
2.4 Multivariable Taylor Series Method	12
CHAPTER 3. Results and discussion	15
3.1 The pH difference between China and the US	15
3.1.1 The pH difference based on observations.	15
3.1.2 The pH difference based on model simulations.	17
3.2 Causes of the aerosol pH difference.	22
3.2.1 Gaseous and particle compounds profiles between China (NCP) and the contiguous US	22
3.2.2 Characterization of contributions to aerosol acidity by individual factors	26
3.2.3 The effect of ammonium on aerosol pH difference	29
3.2.4 The effect of nitrate/sulfate on aerosol pH difference	33
3.2.5 Two pathways leading to the aerosol acidity difference.	37
CHAPTER 4. Conclusions and implications	46
APPENDIX A. Information of monitoring sites used in this study	48
A.1 Information of monitoring sites in the US	48
A.2 Information of monitoring sites in China	49
APPENDIX B. Model evaluation results	50
B.1 Annual mean concentrations of gaseous and aerosol species	50
B.2 Scatter plots of observed values versus simulated values of gaseous and aerosol species.	52
B.3 Monthly trend of gaseous and aerosol species based on observed values and simulated values.	54
REFERENCES	56

## LIST OF TABLES

Table 1 Distribution of observational cases in China in each month (with outliers removed) .....	7
Table 2 Summary of the one-year average values of mass concentration of water-soluble ions (WSI), gaseous and aerosol species, aerosol pH and meteorological parameters (as average $\pm$ standard deviation) in China and the United States during the study periods (i.e., 2017 for China and 2011 for the United States). .....	24
Table 3 Summary of the inputs of Multivariable Taylor Series Method (MTSM) calculation. The unit of concentrations is $\mu\text{g}\cdot\text{m}^{-3}$ , the RH is a relative number with no unit, and the unite of temperature is K. The values in “observation” group are the average values based on observation data, the values in “simulation group” are the average values based on CMAQ simulation data and the “Simulation, population-weighted” group is the population-weighted values based on CMAQ simulation data.....	26

## LIST OF FIGURES

Figure 1	Location of monitoring sites used in this study.....	4
Figure 2	Comparison of results in pH calculation when using different methods to estimate HCl concentration in the United States. ....	6
Figure 3	Observed $\varepsilon(\text{NH}_4^+)$ (left column) and $\varepsilon(\text{NO}_3^-)$ (right column) in China (top row) and the United States (bottom row) versus simulated by ISORROPIA-II. ....	12
Figure 4	Annual average aerosol pH at each monitoring site in China and the United States based on observational data.....	16
Figure 5	The cumulative distribution function (CDF) curves of aerosol pH in China and the United States .....	16
Figure 6	Overlay of annual mean pH calculated based on simulated concentrations (colored map) and observed concentrations (colored dots) over the study domain .....	18
Figure 7	Monthly average values of pH, $\varepsilon(\text{NO}_3^-)$ and $\varepsilon(\text{NH}_4^+)$ based on observed and CMAQ simulated data in China (a, c, e) and in the United States (b, d, f) .....	20
Figure 8	Annual average values of water-soluble ions (WSI) concentration profiles in China (left) and in the United States (right).....	25
Figure 9.	Contributions of individual components and meteorological factors to (a) total difference of aerosol pH ( $\Delta\text{pH}$ ), (b) the aerosol pH difference through the pathway of LWC ( $\Delta\text{pHLWC}$ ), and (c) the aerosol pH difference through the pathway of $\text{H}^+_{\text{air}}$ ( $\Delta\text{pHHair} +$ ) between China and the United States .....	28
Figure 10.	Responses of pH, $\varepsilon(\text{NH}_4^+)$ and $\varepsilon(\text{NO}_3^-)$ to the change of $\text{TNH}_3$ from 0.1 to 1000 $\mu\text{g}\cdot\text{m}^{-3}$ while keep all other components constant at their annual average levels.. ..	31
Figure 11	Distribution of aerosol pH in three groups with different relative abundance of ammonia in two countries.....	33
Figure 12	Values of pH, liquid water content and $\text{H}^+_{\text{air}}$ to the change of $\text{TSO}_4$ and $\text{TNO}_3$ concentration in China and the United States. ....	34
Figure 13	Relation between aerosol pH and $\text{TSO}_4/\text{TNO}_3$ molar ratio in China (left) and the United States (right) based on observational data.....	34
Figure 14	Values of pH, LWC, $\text{H}^+_{\text{air}}$ , $\varepsilon(\text{NH}_4^+)$ , $\varepsilon(\text{NO}_3^-)$ and dissolved mass in group N and group S under different RH conditions in China and the United States. ....	36
Figure 15	Step-specific contributions of individual factors to the pH difference between China and the US. ....	40
Figure 16.	Sensitivity tests showing the pH changes in response to different levels of $\text{SO}_4$ and $\text{TNO}_3$ in an $\text{NH}_4^+-\text{SO}_4^{2-}-\text{NO}_3^--\text{H}_2\text{O}$ system.....	42
Figure 17	Contributions of individual components and meteorological factors to (a) total difference of aerosol pH ( $\Delta\text{pH}$ ), (b) through the pathway of LWC ( $\Delta\text{pHLWC}$ ), (c) through the pathway of $\text{H}^+_{\text{air}}$ ( $\Delta\text{pHHair} +$ ) between the NCP scenario and the US-SE scenario in Zheng’s study (Zheng et al., 2020).....	44

## SUMMARY

Aerosol acidity governs several key processes in aerosol physics and chemistry, thus affecting aerosol mass and composition, and ultimately the climate and human health. Previous studies have reported aerosol pH values separately in China and the United States (US), implying different aerosol acidity between these two countries. However, there is debate about whether mass concentration or chemical composition is the more important driver of differences in aerosol acidity. A full picture of the pH difference and the underlying mechanisms responsible for it is hindered by the scarcity of simultaneous measurements of particle composition and gaseous species, especially in China. Here we conduct a comprehensive assessment of aerosol acidity based on annual mean data in China and the US using extended ground-level measurements and regional chemical transport model simulations. We show that annually aerosol in China is significantly less acidic than in the US, with pH values 1–2 units higher. Based on a proposed multivariable Taylor Series method and a series of sensitivity tests, we identify major factors that potentially leading to the pH difference. Compared to the US, China has much higher aerosol mass concentrations (gas + particle, by a factor of 8.4 on average) and a higher fraction of total ammonia (gas + particle) in the aerosol composition. Our assessment shows that such differences in mass concentrations and chemical composition play equally important roles in driving the aerosol pH difference between China and the US. Therefore, both the facts that China is more polluted than the US and is rich in ammonia together explain the aerosol pH difference. The difference in aerosol acidity

highlighted in the present study implies potential differences in formation mechanisms, physicochemical properties, and toxicity of aerosol particles in these two countries.

## CHAPTER 1. INTRODUCTION

As an intrinsic aerosol property, aerosol acidity (usually characterized by aerosol pH) plays an important role in a variety of aerosol physical and chemical processes (Pye et al., 2020). Aerosol acidity can modulate aerosol mass by controlling the gas-particle partitioning of volatile and semi-volatile acids (such as  $\text{HCl-Cl}^-$  and  $\text{HNO}_3\text{-NO}_3^-$ ) (Guo et al., 2016) and can influence production rates of secondary aerosol through heterogeneous pathways (Jang et al., 2002; Surratt et al., 2010; Pathak et al., 2011). Acidity also affects aerosol optical properties via proton dissociation of organic functional groups (Mo et al., 2017) and the morphology or phase state of organic aerosols (Losey et al., 2016; Losey et al., 2018). Recent evidence links aerosol acidity to aerosol toxicity and health outcomes. For example, highly acidic aerosols cause greater dissolution of metals which can generate reactive oxygen species in vivo (Fang et al., 2017). High aerosol acidity is associated with increased risks of respiratory disease and cancer (Kleinman et al., 1989; Gwynn et al., 2000; Behera et al., 2015).

Due to the difficulties in directly measuring aerosol pH (Jang et al., 2002; Li and Jang, 2012), thermodynamic models, including ISORROPIA-II (Fountoukis and Nenes, 2007), E-AIM (Clegg et al., 1998), and SCAPE2 (Kim and Seinfeld, 1995), have been widely used to calculate aerosol pH based on measured gaseous and particle composition and meteorological data such as relative humidity (RH) and temperature. Multiple studies suggest that these models can reproduce the partitioning of semi-volatile species including  $\text{HNO}_3\text{-NO}_3^-$  and  $\text{NH}_4^+\text{-NH}_3$ , which are sensitive to aerosol pH (Guo et al., 2015; Hennigan et al., 2015; Guo et al., 2016).

Analyses of field observations in different regions of the United States (US) have indicated that aerosol acidity is typically high. For example, Weber et al. (2016)(Weber et al., 2016) showed that aerosol pH in the southeastern US was buffered to be consistently in the range of 0-2 despite a substantial sulfate reduction over the past 15 years, and the same trend may be applicable to other regions. Studies in the northeastern US and California also found highly acidic aerosols with mean pH values of 0.8 and 1.9, respectively (Guo et al., 2017a). Aerosol pH in the midwestern US was typically higher than other areas, with an average of 3.8 (Lawal et al., 2018). Studies in China, on the other hand, have found generally higher aerosol pH. Several studies in the heavily polluted North China Plain (NCP) region reported average pH of 3.5–5.2 (Shi et al., 2017;Ding et al., 2019;Shi et al., 2019;Song et al., 2019;Wang et al., 2020a). Xi'an, a city in northwest China, had aerosol pH values up to 5 (Wang et al., 2016;Guo et al., 2017b). Some sites in southeast China had lower aerosol pH, such as the site in Guangzhou which had an average of 2.3 (Jia et al., 2020). A comprehensive, nationwide comparison of aerosol pH between China and the US can provide a better understanding of the factors driving aerosol pH and its effect on aerosol formation mechanisms and properties (Pathak et al., 2009;Guo et al., 2017a;Wang et al., 2020a). However, such comparisons are still scarce (Guo et al., 2017b;Nenes et al., 2020;Zheng et al., 2020), primarily because of a lack of extensive simultaneous measurements of aerosol composition and semi-volatile gaseous compounds in China.

In this study, we compared the aerosol mass concentrations, chemical composition, and acidity between China and the US based on one-year measurements from 34 ground monitoring sites in the US and 16 sites in China (mostly clustered in the NCP). In order

to extend the spatial coverage to nationwide scales, we employed the Community Multiscale Air Quality (CMAQ) model to simulate the concentrations of gaseous and particle species which were used to calculate aerosol pH across both countries. We confirmed the significant difference in aerosol pH between two countries based on both observational data and simulated data. We proposed a new method to identify the factors driving the pH difference between these two countries and we identified the large effect on  $\text{TNH}_3$  and  $\text{SO}_4$ , though their effect is opposite to each other. We discussed the causes and implications of the pH difference.

## CHAPTER 2. DATA COLLECTION AND STUDY METHOD

### 2.1 Observational data

Measurements of gaseous species (including  $\text{HNO}_3$ ,  $\text{NH}_3$  and  $\text{HCl}$ ) and particle components (including  $\text{SO}_4^{2-}$ ,  $\text{NO}_3^-$ ,  $\text{NH}_4^+$ ,  $\text{Cl}^-$ , and nonvolatile cations (NVCs)) from monitoring networks in China and the US are used for analysis and comparison in this study. NVCs considered are  $\text{Na}^+$ ,  $\text{Mg}^{2+}$ ,  $\text{K}^+$ , and  $\text{Ca}^{2+}$ . The names and locations of the monitoring sites in the US and in China can be found in Tables A1 and A2 in appendix A, respectively. The sum of total observed aerosol ionic compounds is defined as water soluble ions (WSI), though it is recognized that not all of the ions are routinely measured (e.g., trace species and organic ions). We also study the partitioning of semi-volatile species including  $\text{NH}_3$ - $\text{NH}_4^+$  and  $\text{HNO}_3$ - $\text{NO}_3^-$  because they are sensitive to pH, especially when the partitioning ratios,  $\varepsilon(\text{NH}_4^+)$  and  $\varepsilon(\text{NO}_3^-)$ , defined as the molar ratio of  $\text{NH}_4^+$  to total ammonia ( $\text{TNH}_3=\text{NH}_3+\text{NH}_4^+$ ) and the molar ratio of  $\text{NO}_3^-$  to total nitrate ( $\text{TNO}_3=\text{HNO}_3+\text{NO}_3^-$ ), are around 50% (Guo et al., 2017a;Chen et al., 2019).

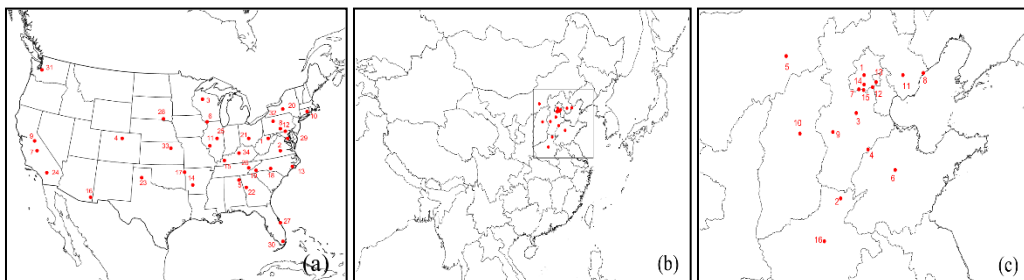


**Figure 1** Location of monitoring sites used in this study in the United States (a) and China (b), with a close-up North China Plain (c).

In the US, observational data are from co-located Clean Air Status and Trends Network (CASTNET) (<https://www.epa.gov/castnet>) and Ammonia Monitoring Network (AMoN) (<http://nadp.slh.wisc.edu/amon/>) sites. CASTNET and AMoN sites are assumed to be co-located if they are within 1km of one another. Observations from co-located sites are then combined for pH calculation. Weekly ambient concentrations of gases and particulate species, including  $\text{HNO}_3$ ,  $\text{SO}_4^{2-}$ ,  $\text{NO}_3^-$ ,  $\text{NH}_4^+$ ,  $\text{Cl}^-$  and NVCs, are available from CASTNET sites, while biweekly concentrations of  $\text{NH}_3$  are available from AMoN sites. To match biweekly data of  $\text{NH}_3$  from AMoN to weekly data of other species from CASTNET, the same  $\text{NH}_3$  are used for both weeks of the CASTNET samples. This assumption is expected to have a minor effect on pH estimates, as a previous study found that a 10 times increase in  $\text{NH}_3$  is required to increase pH by one unit (Guo et al., 2017b). This assumption is also supported in later discussion (Section 3.2.3). HCl data is not available, so we use particle phase  $\text{Cl}^-$  as total Cl for pH calculations. Sensitivity tests assuming HCl concentrations of four times the  $\text{Cl}^-$  concentrations or using HCl concentrations derived from CMAQ modeled HCl/ $\text{Cl}^-$  ratios show little difference in aerosol pH compared to the pH estimated by using particle phase  $\text{Cl}^-$  as total Cl (Figure 2). Considering the reported small change in aerosol pH in the US over a long-term period (Weber et al., 2016; Lawal et al., 2018) and the configuration of the chemical transport model which is set up for the year 2011 (see the following section), we use observational data in 2011 to investigate the aerosol pH in the US. Only sites with measurements available for all species were selected for this study. There are 34 co-located CASTNET and AMoN sites, which are scattered across the contiguous US (Figure 1a). The accuracy of CASTNET measurements has been assessed through the

analysis of reference and continuing calibration verification samples with a criterion of 95-105% (except  $\text{NH}_4^+$ , whose accuracy criterion is 90-110%). Detailed information about data quality is available in the CASTNET Quality Assurance Report-Annual 2011 (United States Environmental Protection Agency, 2012a). A previous study demonstrated that the  $\text{NH}_3$  concentrations measured by the passive AMoN samplers are comparable to annular denuder systems (as a reference system) with a mean relative percent difference of -9% (Puchalski et al., 2015).

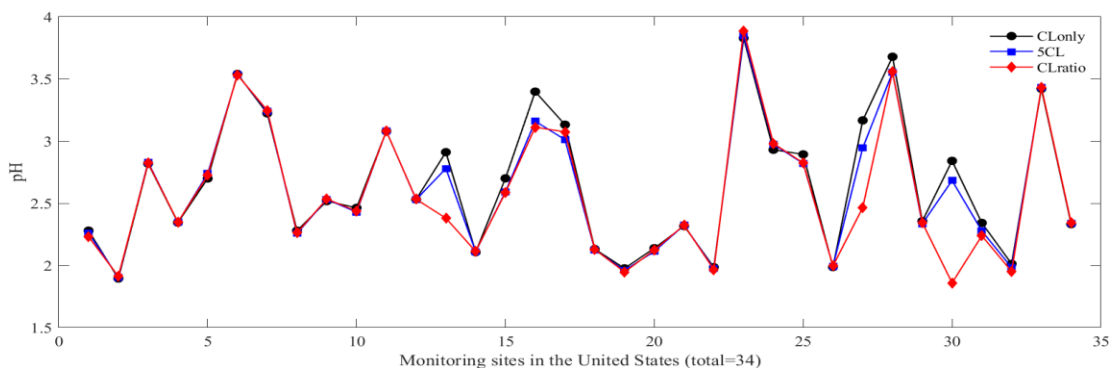


**Figure 2 Comparison of results in pH calculation when using different methods to estimate HCl concentration in the United States. Group “Cl only” means using particle Cl- concentration as total Cl and ignore gas phase HCl; group “5Cl” means assuming total Cl equals to 5 times particle Cl- concentration therefore HCl concentration equals to 4 times particle Cl- concentration; group “Cl ratio” means using measured particle Cl- concentration divided by CMAQ simulation partitioning ratio to estimate the amount of total Cl. The result showed the three methods will lead to essentially the same pH at most of the monitoring sites.**

In China, hourly observational data are extracted from the data-sharing platform operated by the Comprehensive Observation Network for Air Pollution in Beijing-Tianjin-Hebei and its Surrounding Areas (<http://123.127.175.60:8765/siteui/index>). This collaborative observation network is supported by multiple institutions and provides simultaneous observations of gaseous and particle species at individual monitoring sites (Wang et al., 2019). We derive daily average concentrations of gaseous species including  $\text{NH}_3$ ,  $\text{HNO}_3$

and HCl and of particle species including  $\text{NH}_4^+$ ,  $\text{NO}_3^-$ ,  $\text{Cl}^-$ , and NVCs from hourly observational data at 16 monitoring sites for use in pH calculation. These monitoring sites are clustered in NCP in eastern China (Figure 1c). Due to the lack of data quality information, we first process the data by removing unreasonable data points. We define a set of valid data containing all the measured components in one day as one case. We first remove cases with one or more missing components. In this step, 2704 of 5840 cases are removed. We then identify data points that are more than three median absolute deviations from the median as outliers and remove cases with any component identified as an outlier. Eventually, 1766 cases remain for subsequent analyses. Although we remove many cases in this process, the remaining cases cover most of the days in a year and are evenly distributed by month (Table 1).

**Table 1 Distribution of observational cases in China in each month (with outliers removed)**

Month	Jan.	Feb.	Mar.	Apr.	May	Jun.	Jul.	Aug.	Sep.	Oct.	Nov.	Dec.
Number of cases	104	144	176	157	268	184	182	111	30	45	134	231

It should be noted that the weekly (or longer) duration of the CASTNET samples in the US may lead to biases in the measured concentrations especially for volatile species such as ammonium nitrate. Sickles et al. (1999) conducted a comprehensive comparison of measurements using the CASTNET weekly-duration sampling approach with those using a 24-h-duration sampling approach. Both approaches used filter packs. They found that compared to 24-h sampling, weekly sampling led to low biases of -5%, -5%, and -0.7%, on average, in measured  $\text{HNO}_3$ ,  $\text{NO}_3^-$ , and  $\text{NH}_4^+$ , respectively, and high biases of 4% and 16%, on average, in  $\text{SO}_4^{2-}$  and  $\text{SO}_2$ , respectively. To evaluate the potential biases in the

calculated aerosol pH due to the weekly-duration sampling, we conduct a sensitivity test to adjust the CASTNET-measured concentrations based on the reported average differences between weekly-duration and 24-h-duration samples (Sickles et al., 1999) (Section 3.1.1).

## **2.2 Model configuration**

We use CMAQ version 5.0.2 (United States Environmental Protection Agency, 2014) to simulate gaseous and particle species concentrations and aerosol pH in China and the US. The model domains cover mainland China and the contiguous US with 124×184 and 112×148 horizontal grid cells, respectively. Both are resolved at the 36-km horizontal resolution with 13 vertical layers extending to ~16 km above the ground. In both simulations, gas-phase chemistry is modeled with the CB05 chemical mechanism (Yarwood et al., 2005), and the aerosol thermodynamic equilibrium is modeled with ISORROPIA II (Fountoukis and Nenes, 2007).

The meteorological and emission inputs used to drive the China simulation are adopted from “AiMa”, an online operational air quality forecasting system (Lyu et al., 2017; AiMa Forecast, 2017). In the AiMa modeling system, the meteorological data are generated with the Weather Research and Forecasting (WRF) model (William C. Skamarock 2008) driven by the 0.5-degree global weather forecast products produced by the National Centers for Environmental Prediction (NCEP) Global Forecast System (GFS) (Global Forecast System (GFS) Model). The AiMa emission inventory was compiled and derived by integrating a variety of inventories and utilizing various activity data and has been

continuously updated since its establishment (Lyu et al., 2017). The base year of the current AiMa emission inventory is 2017. For the US simulation, we use WRF-modeled meteorological fields downscaled from the North American Regional Reanalysis (NARR) data (Mesinger et al., 2006) as the meteorological input and the 2011 National Emissions Inventory provided by the US Environmental Protection Agency as the emission input (United States Environmental Protection Agency, 2012b). The base year of the meteorology and emissions is consistent with the year of the measurements in each country (i.e., 2017 for China and 2011 for the US).

In order to evaluate the model performance against observations, we calculate normalized mean bias (NMB) and normalized root-mean-square error (NRMSE) to evaluate the spatial variation of pH, species concentrations and partitioning ratios with equations (1) and (2), where  $C_m$  is the modeled value,  $C_o$  is the observed value,  $N$  is the number of simulation-observation pairs.

$$\text{NMB} = \frac{\sum_1^N (C_m - C_o)}{\sum_1^N C_o} \quad (1)$$

$$\text{NRMSE} = \frac{\sqrt{\frac{\sum_1^N (C_m - C_o)^2}{N}}}{\overline{C_o}} \quad (2)$$

### 2.3 Aerosol pH calculation

In this study, we use the ISORROPIA-II thermodynamic model (Fountoukis and Nenes, 2007) to determine the composition in a  $K^+$ - $Ca^{2+}$ - $Mg^{2+}$ - $NH_4^+$ - $Na^+$ - $SO_4^{2-}$ - $NO_3^-$ - $Cl^-$ - $H_2O$  aerosol system under equilibrium conditions with gas phase precursors. Aerosol pH is calculated based on  $H^+$ <sub>air</sub> and liquid water content (LWC) from ISORROPIA-II output:

$$pH = -\log_{10}(\gamma_{H^+} \cdot H_{aq}^+) = -\log_{10}\left(\frac{1000\gamma_{H^+} \cdot H_{air}^+}{LWC}\right) \quad (3)$$

where  $\gamma_{H^+}$  is the activity coefficient of the hydronium ion which is assumed to be 1 in this study (the binary activity coefficients of ionic pairs, including  $H^+$ , are calculated in ISORROPIA-II),  $H^+$ <sub>aq</sub> (mol·L<sup>-1</sup>) is the hydronium ion concentration in aerosol liquid water,  $H^+$ <sub>air</sub> (μg·m<sup>-3</sup>) is the equilibrium particle hydronium ion concentration per volume air. LWC (μg·m<sup>-3</sup>) in this study only considers the water uptake by inorganic species. The effect of water uptake by organic species on aerosol pH has been found to be minor (Guo et al., 2015).

There are two modes in ISORROPIA-II's calculation, the forward mode and the reverse mode. In the forward mode, the inputs include total concentrations (i.e. gas+particle) of  $TNH_3$ ,  $TNO_3$ ,  $TCl$  ( $HCl+Cl^-$ ),  $SO_4$  and NVCs and meteorological parameters (temperature and RH); in the reverse mode, only the particle phase of compounds and meteorological parameters are needed (Fountoukis and Nenes, 2007). In this study, the ISORROPIA-II model is run in the forward mode for aerosol in metastable state because the concentrations of both gas and particle species are available and also because the reverse mode has been reported to be more sensitive to measurement errors (Hennigan et al., 2015; Song et al., 2018).

We find that there are measurements with unrealistically high  $\text{Ca}^{2+}$  concentrations (such that  $\text{Ca}^{2+}$  is more than  $\text{LWC} \times 0.002$ , i.e., the solubility of  $\text{Ca}^{2+}$  in aerosol liquid water). This may be due to the measurement method of  $\text{Ca}^{2+}$  which uses large amounts of water to dissolve filter-collected particles. This process will likely dissolve the water-insoluble part of  $\text{Ca}^{2+}$  in aerosols which may cause higher bias in aerosol  $\text{Ca}^{2+}$  concentrations. In the existence of aerosol  $\text{SO}_4^{2-}$ ,  $\text{Ca}^{2+}$  precipitates along with  $\text{SO}_4^{2-}$  as  $\text{CaSO}_4$  because of the low solubility (Seinfeld and Pandis, 2006). Including the high  $\text{Ca}^{2+}$  concentration leads to large differences in estimated pH because of the high acidity of  $\text{SO}_4^{2-}$  (Section 3.2.4). In order to avoid this potential bias, we use modified  $\text{Ca}^{2+}$  concentration for pH calculations while keeping  $\text{SO}_4^{2-}$  unchanged. That is, we use the original  $\text{Ca}^{2+}$  concentration to calculate aerosol LWC and then use the concentration of  $\text{Ca}^{2+}$  that can dissolve in the LWC as the modified  $\text{Ca}^{2+}$  concentration in cases where the original  $\text{Ca}^{2+}$  exceeds its solubility in the calculated LWC.

We compare the directly measured gas-particle partitioning ratios of semi-volatile compounds with the ratios re-partitioned by ISORROPIA-II using measured total (gas+particle) concentrations as inputs. The purpose of this comparison, as conducted in previous studies (Guo et al., 2016; Guo et al., 2017a), is to examine the measurement data quality. This method is effective when the species have substantial fractions in both gas and particle phases (Guo et al., 2017a). The comparison results of  $\epsilon(\text{NH}_4^+)$  and  $\epsilon(\text{NO}_3^-)$  are shown in Figure 3. The correlation coefficients and the slopes of linear regression are all close to 1, suggesting good agreement between the measured and ISORROPIA-re-calculated partitioning ratios. In terms of these partitioning ratios, the model (ISORROPIA-II) performs better in the US than in China, which may be attributable, in part, to the more

balanced partitioning of the species between gas and particle phase in the US because the partitioning is most sensitive to pH when partitioning ratio is close to 0.5.

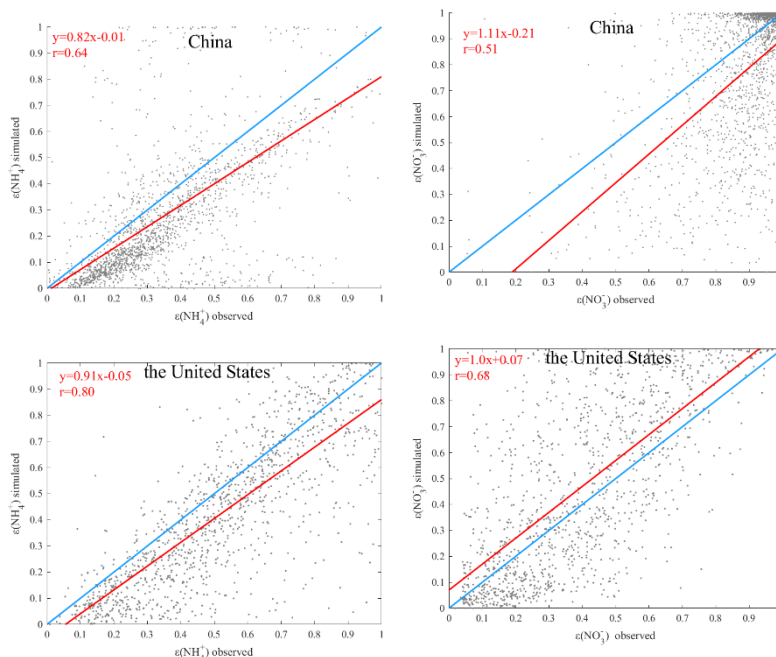


**Figure 3 Observed  $\epsilon(\text{NH}_4^+)$  (left column) and  $\epsilon(\text{NO}_3^-)$  (right column) in China (top row) and the United States (bottom row) versus simulated by ISORROPIA-II. The regression line (red), 1:1 line (blue), and the regression equation and correlation coefficient  $r$  are shown on each panel.**

$$\epsilon(\text{NH}_4^+) = \frac{[\text{NH}_4^+]}{[\text{NH}_4^+] + [\text{NH}_3]}$$

## 2.4 Multivariable Taylor Series Method

To separate the contribution of individual components (eight species in total, including  $\text{Na}^+$ ,  $\text{SO}_4$ ,  $\text{TNO}_3$ ,  $\text{TNH}_3$ ,  $\text{TCl}$ ,  $\text{Ca}^{2+}$ ,  $\text{K}^+$ , and  $\text{Mg}^{2+}$ ) and meteorological variables (RH and temperature) to the pH difference between China and the US, we propose a multivariable Taylor Series method (MTSM). First, we derive the average conditions (i.e., species concentrations and meteorological conditions) across all the sites in the US and China.

We then use the US as the starting point and China as the end point and decompose the contributions of individual compounds to the pH difference based on the following equations:

$$\Delta c_i = c_{i,China} - c_{i,US} \quad (4)$$

$$c_{i,\lambda} \cong c_{i,US} + \Delta c_i \cdot \lambda \quad (5)$$

$$\Delta pH = pH_{US} - pH_{China} = \int_0^1 \left( \sum_{i=1}^8 \frac{\partial pH}{\partial c_{i,\lambda}} \cdot \Delta c_i \right) \cdot d\lambda \cong \sum_{s=1}^{100} \left( \sum_{i=1}^8 \frac{\partial pH}{\partial c_{i,\frac{s}{100}}} \cdot \Delta c_i \right) \cdot 0.01 \quad (6)$$

$$\Delta pH_i \cong \sum_{s=1}^{100} \frac{\partial pH}{\partial c_{i,\frac{s}{100}}} \cdot \Delta c_i \cdot 0.01 \quad (7)$$

where subscript  $i$  denotes a specific species or meteorological variable;  $c_{i,China}$  and  $c_{i,US}$  represent the values of  $i$  in China and the US, respectively;  $\Delta c_i$  is the difference in  $c_i$  between China and the US;  $c_{i,\lambda}$  is an intervening  $c_i$  between  $c_{i,China}$  and  $c_{i,US}$  defined by  $\lambda$ ,  $\lambda \in [0, 1]$ ; when  $\lambda$  is 0,  $c_{i,\lambda}$  is  $c_{i,US}$ ; when  $\lambda$  is 1,  $c_{i,\lambda}$  is  $c_{i,China}$ . The pH difference between China and the US (i.e.,  $\Delta pH$ ) can be expressed as the sum of the partial derivatives of pH with respect to  $c_{i,\lambda}$  which is then integrated from  $c_{i,US}$  to  $c_{i,China}$ , as described by Eq. (6). In this study, we take 100 steps with equal intervals to gradually change  $\lambda$  from 0 to 1 (Eq. (6)) and record the partial derivatives of pH with respect to individual  $c_{i,\lambda}$ , and derive the contributions of all the species and meteorological variables to the pH change at every step. By summing up the contributions of individual variables at all steps, we characterize the contributions of individual factors to the overall pH difference (Eq. (7)). Based on the same method, we further quantify the contributions of individual factors to the

differences in LWC and  $H_{\text{air}}^+$ , respectively, the two variables directly used to calculate aerosol pH (Section 3.2.5).

## CHAPTER 3. RESULTS AND DISCUSSION

### 3.1 The pH difference between China and the US

#### 3.1.1 *The pH difference based on observations.*

The sensitivity test to adjust the CASTNET-measured concentrations based on the reported average differences between weekly-duration and 24-h-duration samples shows little difference between the unadjusted and adjusted pH values in the US ( $2.69 \pm 0.85$  and  $2.74 \pm 0.83$  on average for the unadjusted and adjusted pH, respectively), suggesting that the weekly duration of the CASTNET sampling has little impact on the calculated aerosol pH. Therefore, we proceed with our subsequent analyses using the unadjusted pH. The aerosol pH values calculated based on observational data show a significant difference between China (most observation sites are in NCP) and the US. In China (mainly the NCP), the 2017 annual average pH at monitoring sites is 4.3, ranging from 3.3 to 5.4 with an interquartile range of 3.9–4.6. In the contiguous US, the 2011 annual average pH is 2.6, ranging from 1.9 to 3.9 with an inter-quartile range of 2.2–3.0 (Figure 4). The t-test shows a statistically significant difference between the two groups ( $p < 0.0001$ ), suggesting that the aerosols are on average more acidic at the monitoring sites in the contiguous US than in China (NCP).

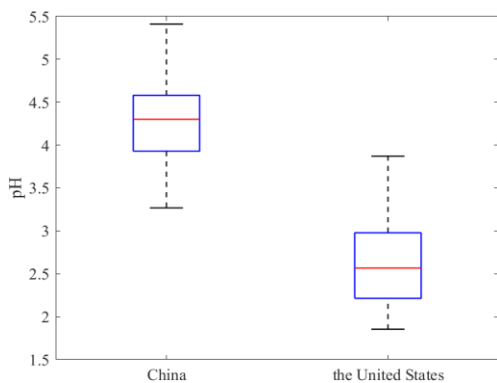


**Figure 4 Annual average aerosol pH at each monitoring site in China and the United States based on observational data. The arithmetic mean (midline), the interquartile range (box), and the minimum-maximum range (whiskers) are shown in the box plot.**

The pH difference is also illustrated by the cumulative distribution function (CDF) curves (Figure 5, solid lines). The shapes of the CDF curves are similar in these two countries with a slightly steeper slope in the contiguous US (Figure 5 a). The pH values, however, are 1–2 units higher in China (NCP) than in the contiguous US across varying levels of cumulative frequencies in the CDF curves. In some cases, aerosols could be completely neutral in China (NCP) (the frequency is 2% for  $\text{pH} \geq 7$ ), while in the contiguous US, the pH values in all cases are below 6.

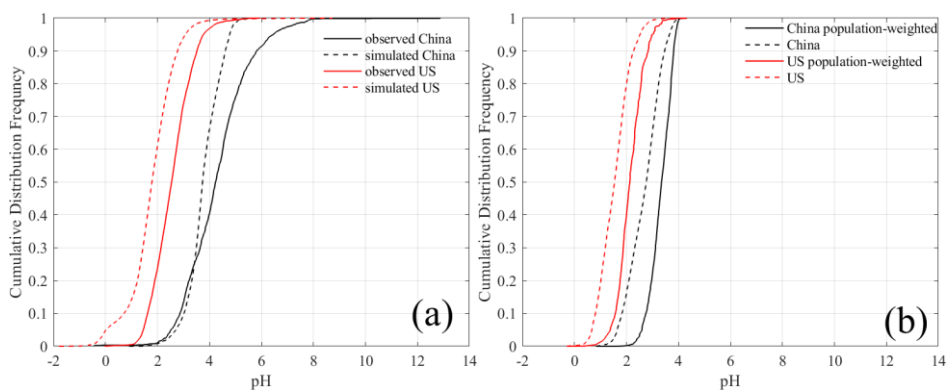


**Figure 5 The cumulative distribution function (CDF) curves of aerosol pH in China and the United States based on (a) observed particulate and gaseous composition**

**(solid lines) and CMAQ simulations collocated with observation sites (dashed line); (b) simulated data nationwide. In panel (b), both average and population weighted CDFs are shown.**

Spatially, 14 out of the 16 sampling sites in China are in the NCP (Figure 1c) which is one of the most populous and polluted regions in China (Hu et al., 2014;Cui et al., 2020). Our pH results in this region are consistent with other studies (ranging from 3.5 to 4.6) (Liu et al., 2017;Ding et al., 2019;Ge et al., 2019). The distribution of sampling sites in the US, on the other hand, is more evenly distributed spatially. The pH values in the Midwest and California are higher than in other regions like the Southeast, in line with previous studies (Lawal et al., 2018;Chen et al., 2019). Overall, the pH level in the US is 1.7 units lower than over the NCP of China.

### *3.1.2 The pH difference based on model simulations.*

To address the issue of insufficient spatial coverage of the observational data in China, we conduct simulations using CMAQ, in conjunction with the observational data, to further study the pH difference on a nationwide scale. We evaluate the model performance by comparing the modeled and observed aerosol pH values (Figure 6), major particle and gaseous species including  $\text{SO}_4^{2-}$ ,  $\text{NO}_3^-$ ,  $\text{NH}_4^+$  and  $\text{HNO}_3$ ,  $\text{NH}_3$ , and the partitioning ratios including  $\epsilon(\text{NH}_4^+)$  and  $\epsilon(\text{NO}_3^-)$ , at monitoring sites (Figures B1-B3 in Appendix B).

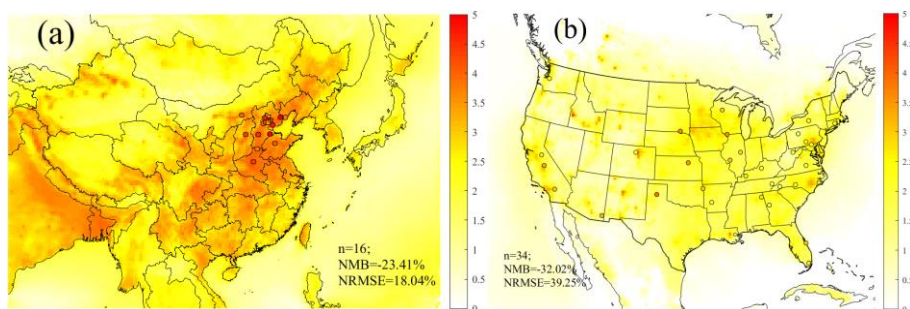


**Figure 6 Overlay of annual mean pH calculated based on simulated concentrations (colored map) and observed concentrations (colored dots) over the study domain in (a) China and (b) the United States. Number of sites (N), normalized mean bias (NMB) and normalized root-mean-square error (NRMSE) are provided in each figure.**

Spatially, the model simulations generally capture the observed variations in pH, species concentrations, and partitioning ratios, although there are some notable biases (Figures B1 and B2). In both China (NCP) and the contiguous US, the modeled  $\text{NH}_4^+$ ,  $\text{NO}_3^-$ , and  $\text{NH}_3$  are biased low while modeled  $\text{HNO}_3$  is biased high, resulting in low biases in the predicted  $\epsilon(\text{NO}_3^-)$  and  $\epsilon(\text{NH}_4^+)$ . The modeled  $\text{SO}_4^{2-}$  in both countries is biased low. Such low biases have been seen in previous studies (Fountoukis et al., 2013;Theobald et al., 2016) and have been attributed to the spatial mismatch between the observations and simulations due to the coarse resolutions of model grid cells (usually 20–50 km resolution) (Shen et al., 2014;Wang et al., 2014a). Smaller NMBs in the US indicate a better performance, compared to China (NCP). Larger differences between observations and simulations in China (NCP) could also be caused by larger measurement uncertainties as the data in China are collected from different monitoring stations operated by individual research institutions (Wang et al., 2019) and thus lack a unified quality control, compared with data in the US, which come from national monitoring networks (United States Environmental Protection Agency;National Atmospheric Deposition Program). The co-occurrence of low biases in  $\epsilon(\text{NO}_3^-)$ , which causes lower

bias in aerosol pH, and low biases in  $\epsilon(\text{NH}_4^+)$  and  $\text{SO}_4^{2-}$ , which cause higher bias in aerosol pH, likely offset each other, resulting in small biases in aerosol pH. Indeed, the simulated average pH values at observation sites ( $3.8 \pm 0.2$  in NCP, China and  $1.8 \pm 0.5$  in the contiguous US) are generally in line with the observed averages ( $4.3 \pm 0.5$  in NCP, China and  $2.6 \pm 0.5$  in the contiguous US) (Fig. 3), although the model shows a moderate low bias in both countries. The larger pH difference in the US than in China is likely due to the low bias in  $\text{TNH}_3$  to which the sensitivity of pH is found to be more pronounced in the US than in China (Section 3.2.3).

With respect to the temporal variation, the model captures the seasonal trends of pH,  $\epsilon(\text{NH}_4^+)$ , and  $\epsilon(\text{NO}_3^-)$  in both countries, with lower values in summer and higher values in winter (Figure 7). The lower temperature in winter favors the partitioning toward particle phase for semi-volatile species. Comparison of the seasonal trends of the individual aerosol components shows a better agreement in the US than in China. For example, the simulation in the US captures the trends of almost all components, though it is biased high for  $\text{SO}_4^{2-}$  and  $\text{NH}_4^+$  in summer (Figure B3 b and h); the simulation in China misses the peaks of  $\text{SO}_4^{2-}$  in winter and  $\text{NH}_3$  in summer has high biases for  $\text{HNO}_3$  in summer (Figure B3 a, i, and e). Measurement-related biases may contribute to the disparity in the temporal trends between observed and modeled concentrations. The uncertainty in monthly profiles of emission estimates may also play an important role. For example, CASTNET's long sampling period could lead to a larger measurement bias in summer than in winter (Sickles and Shadwick, 2008); the large uncertainty in the current estimates of  $\text{NH}_3$  emissions in China, especially the reported underestimation of summertime emissions as indicated by an inversion analysis (Kong et al., 2019), may

cause the absence of the summertime  $\text{NH}_3$  peak in the simulated trend (Fig. S6i). Further investigation is needed to better understand the factors underpinning the disparity between observations and model simulations. In spite of the various potential uncertainties, overall, the spatial and temporal evaluation suggests generally good agreement between the model simulations and observations in both countries.

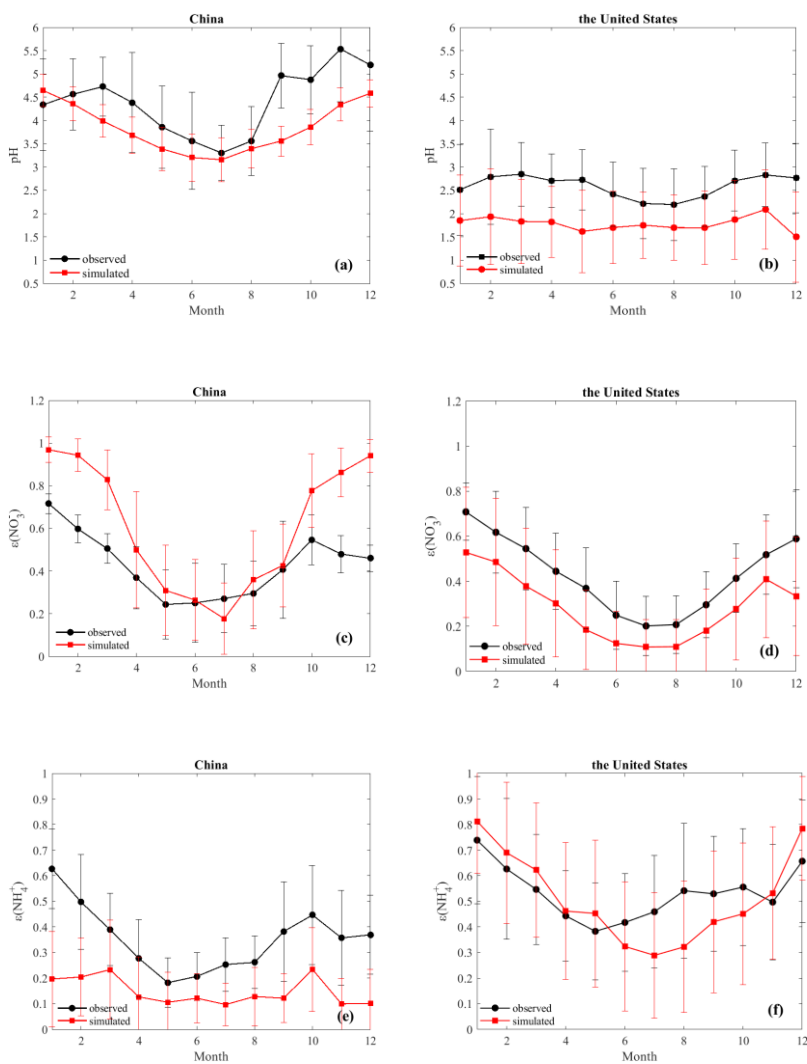


**Figure 7** Monthly average values of pH,  $\epsilon(\text{NO}_3^-)$  and  $\epsilon(\text{NH}_4^+)$  based on observed and CMAQ simulated data in China (a, c, e) and in the United States (b, d, f). The error bars represent the standard deviation of all the cases in each month.

In line with observations (Sect. 3.1.1), the nationwide model simulations show significant differences in aerosol acidity between the two countries. Almost all the areas in the US have aerosol pH values lower than 3 according to the CDF (Figure 5b). Higher pH values are found in the middle and eastern US, while in the western US except California, the pH values are lower (Figure 6). In China, a large portion of areas (87%) have aerosol pH values above 3 according to the CDF. This is especially true in eastern China which has the largest population (Figure 6). Aerosol pH values in western and southeastern China are generally lower than in the east. It should be noted that due to the scarcity of observational data, the pH estimates in southern and western China are not evaluated. The nationwide annual average pH values in China and the US are  $2.7\pm 0.6$  and  $0.8\pm 0.8$  units, respectively, lower than the observation-based values due partly to the model bias but also because most of the monitoring sites are in areas with high pH (Figure 6).

Given the adverse health impacts of ambient aerosols (Burnett et al., 2014; Freedman et al., 2019) and the potential linkage of aerosol acidity with aerosol toxicity through the solubility of redox-active metals (Oakes et al., 2012; Fang et al., 2015; Ye et al., 2018), we further calculate and compare the population-weighted averages of aerosol pH in the two countries to highlight the pH levels in densely populated areas. The population-weighted pH values are  $3.3\pm 0.4$  and  $2.2\pm 0.5$  in China and the US, respectively, both of which are higher than non-weighted averages, indicating that aerosols in more populous areas tend to be less acidic (Figure 5b). This finding is further confirmed by the statistically significant positive correlation ( $\alpha=0.01$ ), within each country, between the aerosol pH and population density (China:  $r=0.42$ ,  $p<0.0001$ ; the US:  $r=0.28$ ,  $p<0.0001$ ). Consistent with the observation-based results, the t-test for the model simulations shows a

significant difference in both the population-weighted and non-weighted aerosol pH values between the two countries ( $p < 0.001$ ).

## **3.2 Causes of the aerosol pH difference.**

### *3.2.1 Gaseous and particle compounds profiles between China (NCP) and the contiguous US*

We further investigate the factors leading to the pH difference. Although both observations and simulations are subject to uncertainty, we expect that observations should provide more direct and reliable evidence for this investigation. It should be noted that the monitoring sites in China were clustered in NCP and, thus, may not be representative of the whole of China. Table 2 summarizes the annual average concentrations of gaseous and particle species measured in China (NCP) and the contiguous US during the study period (China: 2017; US: 2011). For all the gaseous and ionic species (except  $\text{HNO}_3$ ), the average concentrations in China (NCP) are statistically significantly higher than those in the contiguous US. The total concentrations of WSI species in China (NCP) ( $34.4 \mu\text{g}\cdot\text{m}^{-3}$ ) are on average six times the concentrations in the contiguous US ( $5.7 \mu\text{g}\cdot\text{m}^{-3}$ ) and have greater variation, ranging from  $0.2\text{--}240 \mu\text{g}\cdot\text{m}^{-3}$ , compared to a range of  $0.1\text{--}31 \mu\text{g}\cdot\text{m}^{-3}$  in the contiguous US. Similar to other studies in China (Yao et al., 2002; Pathak et al., 2009; Zhang et al., 2013; Liu et al., 2016) and the US (Guo et al., 2015; Feng et al., 2020),  $\text{NH}_4^+$ ,  $\text{NO}_3^-$  and  $\text{SO}_4^{2-}$ , contribute more than 80% of the total WSI concentrations in both countries. The mass fractions of individual WSIs, however, differ between the two countries (Figure 8). In China (NCP), the dominant

WSI was  $\text{NO}_3^-$  (34.6%), followed by  $\text{SO}_4^{2-}$  (26.3%) and  $\text{NH}_4^+$  (25.5%). In the contiguous US in 2011,  $\text{SO}_4^{2-}$  contributed nearly half of the total WSI concentration (49.4%), and the contributions of  $\text{NO}_3^-$  and  $\text{NH}_4^+$  are comparable ( $\text{NO}_3^-$  17.6%,  $\text{NH}_4^+$  18.8%). Note that  $\text{SO}_4^{2-}$  and  $\text{NO}_3^-$  levels have been decreasing dramatically over the years, leading to decreases in  $\text{NH}_4^+$  since there is less substrate to interact with  $\text{NH}_3$  and form particulate ammonium species (Butler et al., 2016).

**Table 2 Summary of the one-year average values of mass concentration of water-soluble ions (WSI), gaseous and aerosol species, aerosol pH and meteorological parameters (as average  $\pm$  standard deviation) in China and the United States during the study periods (i.e., 2017 for China and 2011 for the United States).**

	China(n=1845)	US(n=1191)
<b>WSI (<math>\mu\text{g}\cdot\text{m}^{-3}</math>)</b>	34.4 $\pm$ 25.5	5.7 $\pm$ 2.2
<b>Temperature (K)</b>	284.8 $\pm$ 11.7	287.4 $\pm$ 10.0
<b>RH (%)</b>	45.1 $\pm$ 17.6	71.4 $\pm$ 20.9
<b>pH</b>	4.3 $\pm$ 1.2	2.6 $\pm$ 0.7
<b>Particle phase (<math>\mu\text{g}\cdot\text{m}^{-3}</math>)</b>		
<b>SO<sub>4</sub><sup>2-</sup></b>	9.2 $\pm$ 7.1	2.2 $\pm$ 1.3
<b>NO<sub>3</sub><sup>-</sup></b>	12.1 $\pm$ 11.1	0.8 $\pm$ 0.9
<b>NH<sub>4</sub><sup>+</sup></b>	8.9 $\pm$ 8.0	0.8 $\pm$ 0.5
<b>Cl<sup>-</sup></b>	2.2 $\pm$ 2.3	0.4 $\pm$ 0.1
<b>Na<sup>+</sup></b>	0.7 $\pm$ 1.0	0.2 $\pm$ 0.2
<b>K<sup>+</sup></b>	0.7 $\pm$ 0.6	0.1 $\pm$ 0.1
<b>Ca<sup>2+</sup></b>	1.0 $\pm$ 0.1	0.3 $\pm$ 0.2
<b>Mg<sup>2+</sup></b>	0.2 $\pm$ 0.1	0.1 $\pm$ 0.1
<b>Gaseous phase (<math>\mu\text{g}\cdot\text{m}^{-3}</math>)</b>		
<b>NH<sub>3</sub></b>	18.0 $\pm$ 12.6	1.1 $\pm$ 1.7
<b>HCl</b>	1.9 $\pm$ 3.4	-
<b>HNO<sub>3</sub></b>	1.0 $\pm$ 1.1	1.0 $\pm$ 0.6
<b>Total (<math>\mu\text{g}\cdot\text{m}^{-3}</math>)</b>		
<b>TNH<sub>3</sub></b>	26.5 $\pm$ 17.2	1.9 $\pm$ 1.8
<b>TCl</b>	4.1 $\pm$ 4.5	-
<b>TNO<sub>3</sub></b>	13.1 $\pm$ 11.2	1.8 $\pm$ 1.1

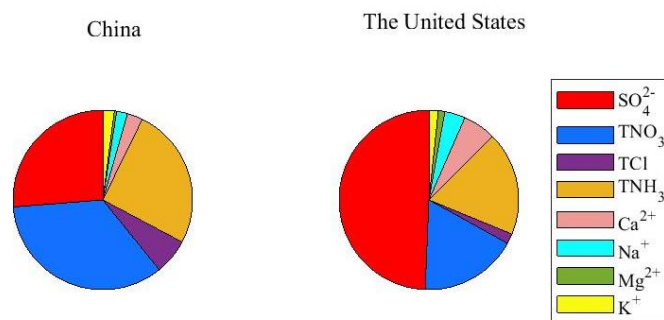


**Figure 8 Annual average values of water-soluble ions (WSI) concentration profiles in China (left) and in the United States (right).**

Two of the most predominant anions in aerosols,  $\text{SO}_4^{2-}$  and  $\text{NO}_3^-$  at the monitoring sites in China (NCP) are present at four and 15 times the concentrations observed in the contiguous US, respectively. The relative difference in  $\text{NO}_3^-$  between the two countries is the most significant, compared with the differences in other WSI components. Hence, the difference of the nitrate to sulfate molar ratio ( $\text{NO}_3^-/\text{SO}_4^{2-}$ ) is also significant between the two countries. The observational data show that the ratios at most monitoring sites in China (NCP) are larger than 1, and that only two sites have ratios lower but close to 1 (0.81, 0.94). On the other hand, 27 out of the 34 sites in the contiguous US show a ratio lower than 1, ranging from 0.25–0.99. High  $\text{NO}_3^-/\text{SO}_4^{2-}$  in China (NCP) could be caused by more efficient oxidation of  $\text{NO}_x$  than  $\text{SO}_2$  in China leading to greater nitrate formation as well as higher aerosol pH and availability of  $\text{NH}_3$  which favor the formation process of particle nitrate (Guo et al., 2018; Vasilakos et al., 2018). The varying ratios of  $\text{NO}_3^-/\text{SO}_4^{2-}$  on aerosol could further affect aerosol liquid water uptake, which is discussed in later section (Section 3.2.4).

The most abundant cation in aerosols is  $\text{NH}_4^+$ , and the concentration difference of  $\text{NH}_4^+$  between the two countries (by a factor of 11) is more significant than the difference of other cations (by factors of 2-7). In addition,  $\epsilon(\text{NH}_4^+)$  in China (NCP) (0.13–0.48) is approximately 50% lower than in the contiguous US (0.22-0.85), meaning that compared to the US,  $\text{TNH}_3$  in China tends to be present more in the gas phase. Higher  $\text{NH}_4^+$  and lower  $\epsilon(\text{NH}_4^+)$  levels in China amount to a higher level of  $\text{TNH}_3$  which has an important influence on aerosol pH, partitioning of  $\text{TNO}_3$  and even particulate mass (see Section 3.2.4 for more discussion).

### 3.2.2 *Characterization of contributions to aerosol acidity by individual factors*

We use MTSM as described in Sect. 2.4 to characterize the contribution of each component to the pH difference between the US and China. Three groups (i.e., observation, simulation non-weighted, simulation population-weighted) of the annual average concentrations in the US and China listed in Table 3 are chosen as the starting (US) and ending (China) points to perform the analysis. The results are shown in Figure 9.

**Table 3 Summary of the inputs of Multivariable Taylor Series Method (MTSM) calculation.** The unit of concentrations is  $\mu\text{g}\cdot\text{m}^{-3}$ , the RH is a relative number with no unit, and the unite of temperature is K. The values in “observation” group are the average values based on observation data, the values in “simulation group” are the average values based on CMAQ simulation data and the “Simulation, population-weighted” group is the population-weighted values based on CMAQ simulation data.

<b>Observation</b>										
	Na <sup>+</sup>	SO <sub>4</sub>	TNH <sub>3</sub>	TNO <sub>3</sub>	TCl	Ca <sup>2+</sup>	K <sup>+</sup>	Mg <sup>2+</sup>	RH	Temp
<b>US</b>	0.16	2.16	1.87	1.75	0.39	0.03	0.07	0.05	0.71	284.75
<b>China</b>	0.69	9.19	26.53	13.11	4.1	0.03	0.72	0.15	0.45	287.39
<b>Simulation</b>										
	Na <sup>+</sup>	SO <sub>4</sub>	TNH <sub>3</sub>	TNO <sub>3</sub>	TCl	Ca <sup>2+</sup>	K <sup>+</sup>	Mg <sup>2+</sup>	RH	Temp
<b>US</b>	0.03	0.85	0.56	0.75	0.11	0.02	0.02	0.01	0.72	285.96
<b>China</b>	0.08	1.95	3.05	2.82	0.11	0.05	0.11	0.02	0.72	280.98
<b>Simulation, population-weighted</b>										
	Na <sup>+</sup>	SO <sub>4</sub>	TNH <sub>3</sub>	TNO <sub>3</sub>	TCl	Ca <sup>2+</sup>	K <sup>+</sup>	Mg <sup>2+</sup>	RH	Temp
<b>US</b>	0.03	1.42	1.79	2.41	0.13	0.03	0.08	0.01	0.66	287.86
<b>China</b>	0.18	3.96	8.41	7.21	0.23	0.09	0.29	0.04	0.7	289.26
<b>Sensitivity test, increasing concentrations with a constant factor and then changing the composition</b>										
	Na <sup>+</sup>	SO <sub>4</sub>	TNH <sub>3</sub>	TNO <sub>3</sub>	TCl	Ca <sup>2+</sup>	K <sup>+</sup>	Mg <sup>2+</sup>	RH	Temp
<b>US, original</b>	0.16	2.16	1.87	1.75	0.39	0.03	0.07	0.05	0.71	284.75
<b>US composition, Chinese level</b>	1.33	18.19	15.74	17.42	3.28	0.22	0.62	0.43	0.71	284.75
<b>China</b>	0.69	9.19	26.53	13.11	4.1	0.03	0.72	0.15	0.71	284.75

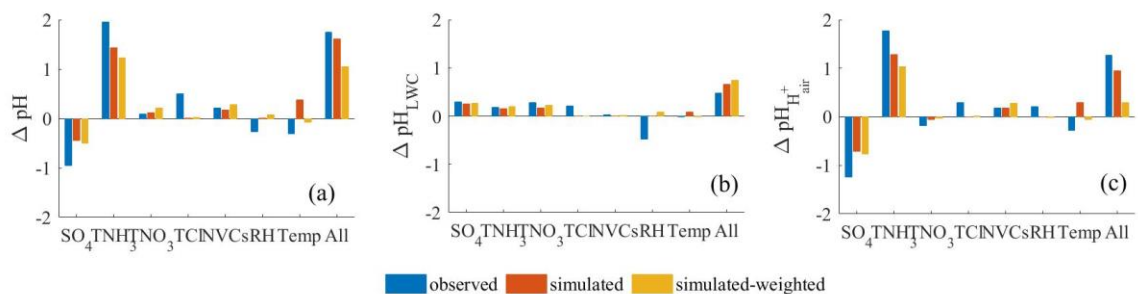


**Figure 9. Contributions of individual components and meteorological factors to (a) total difference of aerosol pH ( $\Delta pH$ ), (b) the aerosol pH difference through the pathway of LWC ( $\Delta pH_{LWC}$ ), and (c) the aerosol pH difference through the pathway of  $H^+_{air}$  ( $\Delta pH_{H^+_{air}}$ ) between China and the United States calculated by multi-variable Taylor series method (MTSM) in Sect. 2.4. For each factor, the sum of the contributions through the two pathways yields the net contribution of this factor to the aerosol pH. The case in the United States is chosen as the starting point, and China as the ending point.**

The average concentrations based on the observational and simulated data are not completely consistent due to the representativeness of the monitoring sites and the discrepancy between the simulations and observations. The MTSM analyses based on the three groups, however, show similar results. For example, all three groups suggest the high TNH<sub>3</sub> in China as an important factor leading to the difference in aerosol pH between the two countries (Figure. 9). The contribution of TNH<sub>3</sub> is the highest in the “observation” group due to the large difference in TNH<sub>3</sub> concentration. Other cations, mainly NVCs, have a relatively small effect (0.2, 0.2, and 0.3 in groups “observation”, “simulation”, “simulation-weighted”, respectively), which is consistent with a previous study (Zheng et al., 2020). Unlike TNH<sub>3</sub> and NVCs which lead to higher pH values in China than in the US, SO<sub>4</sub><sup>2-</sup> contributes in the opposite direction to the pH difference. High SO<sub>4</sub><sup>2-</sup> concentrations decrease aerosol pH in China by 0.6–1.3 units, compared to the US, although this effect is fully offset by TNH<sub>3</sub>.

Compared to other species, the concentrations of  $\text{TNO}_3$  are the most different between the two countries (by a factor of 15), but MTSM shows that the contribution of  $\text{TNO}_3$  to the pH difference is relatively small (0.1, 0.1, and 0.2 in the observation, non-weighted, and population-weighted groups). This result is further confirmed by a sensitivity test of  $\text{TNO}_3$  (Fig. S10) which shows that the change in pH from changing only  $\text{TNO}_3$  is small in both countries.

Studies have identified an important role of temperature in driving aerosol pH (Battaglia et al., 2017; Tao and Murphy, 2019; Jia et al., 2020). Our MTSM analysis shows that temperature accounts for 0.07–0.39 unit of pH difference between China and the US, which varies by group (Figure 9). Such relatively small contributions of temperature, compared to those of  $\text{TNH}_3$  and  $\text{SO}_4$ , are mainly because of the small difference in temperature between these two countries which are at similar latitudes. The difference in the annual average temperature between China and the US is 1.4 K, -5.0 K, and 2.6 K in the observation, non-weighted, and population-weighted groups, respectively (Table 3).

### *3.2.3 The effect of ammonium on aerosol pH difference*

The result of MTSM indicates that the difference in  $\text{TNH}_3$  is one of the predominant reasons causing the pH difference. In order to study the effect of  $\text{TNH}_3$ , we conduct sensitivity tests for China and the US separately to investigate the responses of aerosol pH to changing  $\text{TNH}_3$ . We change the  $\text{TNH}_3$  concentrations from 0.1 to 1000  $\mu\text{g}\cdot\text{m}^{-3}$  while keep all other components constant at their annual average levels based on observation data (Table 3). We also use simulation data with population as the weight to study the effects, which consider other areas in China where  $\text{TNH}_3$  concentration is not as

high as in NCP. The results are shown in Figure. 10. It is clearly illustrated that, over a large range of  $\text{TNH}_3$  concentrations, aerosol pH increases with the increase in  $\text{TNH}_3$  because the production process of  $\text{NH}_4^+$  from  $\text{NH}_3$  consumes aqueous  $\text{H}^+$ . The local sensitivity of pH to  $\text{TNH}_3$ , expressed as the pH increase per tenfold increase in  $\text{TNH}_3$  at current  $\text{TNH}_3$  level, is higher in the US (3.0 based on observational data and 1.6 based on simulation data) than in China (0.4 based on observational data and 1.2 based on simulation data), indicated a higher sensitivity of aerosol pH to  $\text{TNH}_3$  in the US than in China. Besides, we find that the responses of pH to  $\text{TNH}_3$  are nonlinear and anisotropic. With all others equal, pH in the US could be closer to the level in China if the  $\text{TNH}_3$  increases to the level in China. On the other hand, the pH in China would be lower than the US if the  $\text{TNH}_3$  decreases to the US level because of the relative higher abundances of acidic components ( $\text{SO}_4$ ,  $\text{TNO}_3$ ,  $\text{TCl}$ ) than basic ions ( $\text{TNH}_3$ ,  $\text{NVCs}$ ) (Figure 10a). In both countries, the sensitivities would quickly diverge from the original values toward higher values as  $\text{TNH}_3$  decreases, with the sensitivities in China changing at a faster pace. As  $\text{TNH}_3$  increases, however, the sensitivities in these two countries would gradually become constant, stabilizing at comparable levels (0.002 pH unit per  $\text{TNH}_3$  increase in both two countries). Results based on simulation data are similar with results based on observational data, especially the sensitivity of aerosol pH at high level of  $\text{TNH}_3$  (represented by similar slope). Higher pH values in China based on simulation data at low  $\text{TNH}_3$  level ( $1\text{-}10 \mu\text{g}\cdot\text{m}^{-3}$ ) could be caused by lower  $\text{SO}_4^{2-}$  concentrations. However, lower value of aerosol pH at high level of  $\text{TNH}_3$  ( $> 50 \mu\text{g}\cdot\text{m}^{-3}$ ) based on simulation data even with lower  $\text{SO}_4^{2-}$  concentrations indicates the limit effect of  $\text{TNH}_3$  at this level and potential effect of other components.

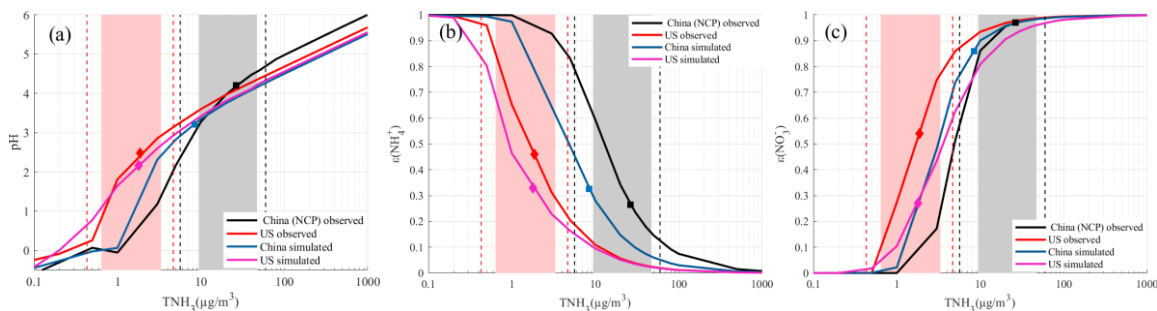


**Figure 10. Responses of pH,  $\epsilon(\text{NH}_4^+)$  and  $\epsilon(\text{NO}_3^-)$  to the change of  $\text{TNH}_3$  from 0.1 to 1000  $\mu\text{g}\cdot\text{m}^{-3}$  while keep all other components constant at their annual average levels.** The shaded areas show the  $\text{TNH}_3$  concentration ranges that covers 75% of the observed cases in the countries, the dashed lines show the 5<sup>th</sup> and 95<sup>th</sup> percentiles of the observed cases, the black square and the red diamond mark the average  $\text{TNH}_3$  levels in China and the United States, respectively.

The effects of  $\text{TNH}_3$  on the gas-particle partitioning of  $\text{NH}_3\text{-NH}_4^+$  and  $\text{HNO}_3\text{-NO}_3^-$  are illustrated in Figure 10b and 10c, showing a decreasing trend of  $\epsilon(\text{NH}_4^+)$  and an increasing trend of  $\epsilon(\text{NO}_3^-)$  as  $\text{TNH}_3$  increases. In the range of observation cases the value of  $\epsilon(\text{NH}_4^+)$  in China is smaller than in the US, suggesting excess presence of  $\text{TNH}_3$  compared to other aerosol components (e.g.,  $\text{TNO}_3$  and  $\text{SO}_4^{2-}$ ). The gas to particle partitioning of  $\text{NH}_3$  produces inorganic ammonium salt of ammonium bisulfate ( $\text{NH}_4\text{HSO}_4$ ) and ammonium sulfate ( $(\text{NH}_4)_2\text{SO}_4$ ) first because the affinity of sulfuric acid for  $\text{NH}_3$  is much larger than that of nitric and hydrochloric acid for  $\text{NH}_3$ , especially when  $\text{TNH}_3$  concentration is relatively low (Behera et al., 2013); The excess  $\text{TNH}_3$  may also react with nitric acid and hydrochloric acid to form salt of  $\text{NH}_4\text{NO}_3$  and  $\text{NH}_4\text{Cl}$  which will dissolve in the aerosol liquid water (Zhao et al., 2016). That is why the increase of  $\epsilon(\text{NO}_3^-)$  is small at the beginning and gradually become faster later. At the same level of  $\text{TNH}_3$ ,  $\epsilon(\text{NH}_4^+)$  in China is higher than  $\epsilon(\text{NH}_4^+)$  in the United States, causing by formation of  $\text{NH}_4\text{NO}_3$  due to higher level of  $\text{TNO}_3$ . Both the lower  $\epsilon(\text{NH}_4^+)$  and higher  $\epsilon(\text{NO}_3^-)$  in China estimated by the sensitivity curves are consistent with observations.

Therefore, the ratio of  $[\text{NH}_4^+]$  to different acid ions ( $[\text{SO}_4^{2-}]$ ,  $[\text{NO}_3^-]$ ,  $[\text{Cl}^-]$ ) can be used to indicate the relative abundance of ammonia. To further investigate the different levels of abundance of ammonia, we tend to look at groups of real cases, instead of the average values only. We divide the observation data into three groups based on neutralization condition of particle phase  $\text{NH}_4^+$ . Group A contains the observations when  $[\text{NH}_4^+] < 2 \times [\text{SO}_4^{2-}]$ , when available  $\text{NH}_4^+$  cannot completely balance aerosol  $\text{SO}_4^{2-}$ . Group B consists of the data points when  $2 \times [\text{SO}_4^{2-}] < [\text{NH}_4^+] < 2 \times [\text{SO}_4^{2-}] + [\text{NO}_3^-] + [\text{Cl}^-]$  when most of the aerosol  $\text{SO}_4$  is in the form of  $\text{SO}_4^{2-}$  and excess  $[\text{NH}_4^+]$  is available to stabilize nitrate and chloride driving the gas phase to shift to the particle phase. Group C contains the data points when  $[\text{NH}_4^+] > 2 \times [\text{SO}_4^{2-}] + [\text{NO}_3^-] + [\text{Cl}^-]$ , where available  $\text{NH}_4^+$  is enough to balance particle phase anions. The distribution of pH values in three groups in two countries is shown in Figure 11 by boxplots. Note that no data in the United States fall in Group C, making up only two groups in Figure 11 (b). Overall, cases in groups B and C with higher relative abundance of ammonia are more likely to have higher aerosol pH than in group A, though the relationship is not linear and does not happen in all the cases. Note that although the relative abundance of  $\text{NH}_4^+$  in group B is smaller than in group C, the transition from group B to group C due to  $\text{TNH}_3$  increase does not always happen. Because if  $\text{TNH}_3$  increase in an aerosol system with  $2 \times [\text{SO}_4^{2-}] < [\text{NH}_4^+] < 2 \times [\text{SO}_4^{2-}] + [\text{NO}_3^-] + [\text{Cl}^-]$ ,  $[\text{NH}_4^+]$  would increase, and more  $\text{TNO}_3$  and  $\text{TCl}$  would shift into the particle phase, leading to the increase of WSI concentration. However, the average WSI concentration in group B is  $55.03 \pm 46.79 \mu\text{g}\cdot\text{m}^{-3}$  in China, significantly higher than that in group C in China ( $31.60 \pm 20.29 \mu\text{g}\cdot\text{m}^{-3}$ ). LWC in group B ( $22.90 \pm 7.38 \mu\text{g}\cdot\text{m}^{-3}$ ) is also higher than that in group C ( $14.37 \pm 16.85 \mu\text{g}\cdot\text{m}^{-3}$ ). We find that most of the cases in group

B could be identified as highly polluted cases where large amount of  $\text{NH}_4\text{NO}_3$  is formed and dissolves in the aerosol water.

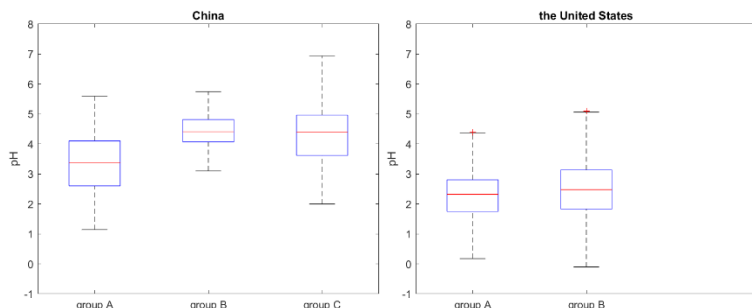


**Figure 11 Distribution of aerosol pH in three groups with different relative abundance of ammonia in two countries. Outliers recognized by data out of the range of three times median absolute deviations from the median are removed.**

Throughout the observed cases, 85% in China are in Group C (i.e., aerosol systems with excess  $\text{NH}_4^+$ ), and 55% in the US are in Group A (i.e., aerosol systems with insufficient  $\text{NH}_4^+$ ). Overall, the positive sensitivity of pH to  $\text{TNH}_3$  and the different dominant groups in these two countries (Group C in China, Group A in the US) suggest that the high abundance of  $\text{TNH}_3$  in China increases the aerosol pH and is one of the major reasons for the pH difference between the two countries.

### 3.2.4 *The effect of nitrate/sulfate on aerosol pH difference*

Besides the effect of  $\text{TNH}_3$  discussed in Sect. 3.2.3, other species, especially the acidic species which mainly include  $\text{SO}_4$  and  $\text{TNO}_3$ , could also affect aerosol pH because of their effects on  $\text{H}^+_{\text{air}}$  concentration as well as on LWC (Ding et al., 2019). This effect is investigated in a sensitivity test by changing  $\text{TNO}_3$  or  $\text{SO}_4$  concentration while keeping other inputs constant as the average levels (Figure 12). Similar to the MSTM results as

shown in Figure 9, elevated  $\text{SO}_4^{2-}$  significantly increases aerosol acidity by increasing  $\text{H}^+_{\text{air}}$ . On the other hand, elevated  $\text{TNO}_3$  only slightly increases  $\text{H}^+_{\text{air}}$ , indicating a weaker acidity than that of  $\text{SO}_4^{2-}$ , in line with the result in a previous study (Guo et al., 2017b). This is partially due to the semi-volatile property of  $\text{TNO}_3$  (Ding et al., 2019). Notably, even in China where  $\epsilon(\text{NO}_3^-)$  are mostly close to 1, the variation of aerosol pH with  $\text{TNO}_3$  (roughly equals to  $\text{NO}_3^-$  in this case) is also subtle. Therefore, for two systems with different moles of  $\text{SO}_4^{2-}$  and  $\text{NO}_3^-$  neutralized by same moles of  $\text{NH}_4^+$ , the system with more  $\text{SO}_4^{2-}$  will likely have a lower pH. This result indicates that higher aerosol acidity is associated with higher availability of  $\text{SO}_4^{2-}$  rather than  $\text{TNO}_3$ , which can be confirmed by observed data in Figure 13.

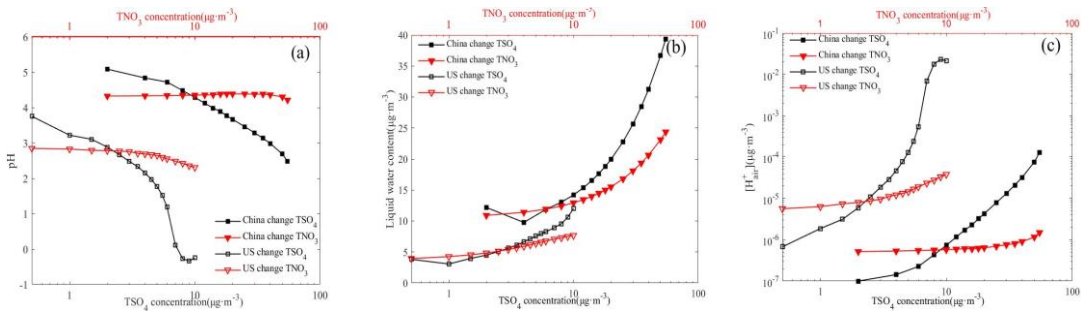


**Figure 12 Values of pH, liquid water content and  $\text{H}^+_{\text{air}}$  to the change of  $\text{TSO}_4$  and  $\text{TNO}_3$  concentration in China and the United States.**

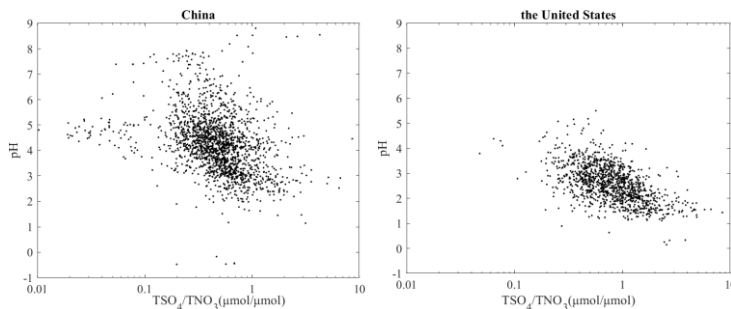


**Figure 13 Relation between aerosol pH and  $\text{TSO}_4/\text{TNO}_3$  molar ratio in China (left) and the United States (right) based on observational data.**

Based on observation data, 74.5% of the cases in China have  $\text{NO}_3^-/\text{SO}_4^{2-}$  molar ratio larger than one, while only 22.3% in the US. The different  $\text{NO}_3^-/\text{SO}_4^{2-}$  ratios, could subsequently affect other aerosol properties, such as aerosol water uptake ability, which is one of the important reasons causing haze events in China during wintertime (Xie et al., 2019; Wang et al., 2020b). Although nitrate aerosol and sulfate aerosol absorbs similar amounts of water per mass, heavy haze events in China are usually associated with increased LWC with enhanced RH levels under nitrate-dominant condition (Wang et al., 2020b).

In order to study this effect, we categorize the observation data into a nitrate-rich group (Group N, where  $[\text{NO}_3^-]/[\text{SO}_4^{2-}] > 3$ ) and a sulfate-rich group (Group S, where  $[\text{NO}_3^-]/[\text{SO}_4^{2-}] < 1$ ) and compare these two groups under different RH conditions. The ratio 3 in group N is mentioned in lab studies and is a more typical value of nitrate-rich conditions in field observations (Ge et al., 1998; Xie et al., 2019).

The results in Figure 14 show that aerosol pH values in the same groups in China and the US have similar responses to the changes in RH. In both countries, as RH increases, the pH in group N decreases, and the pH in group S increases (Figure 14). Both the values and the increasing rate of LWC in group N is larger than in group S, suggesting a higher water uptake ability in nitrate-rich condition, which is likely due to higher aerosol mass compared with group S as shown in Figure 14. The nearly two times aerosol mass in group N as in group S indicates the co-condensation effect of nitrate aerosol and LWC (Guo et al., 2017a), which suggests that  $\text{NO}_3^-$  formed in aerosol leads to a higher LWC due to the increase in aerosol mass, while higher LWC dilutes  $\text{H}^+_{\text{air}}$  and increases pH, which is favorable for more  $\text{HNO}_3$  shifting from gas phase to particle phase and thus

continually increases particle  $\text{NO}_3^-$  concentration. This effect will reach a balance when most of the gas phase  $\text{HNO}_3$  is in the particle phase with enough  $\text{NH}_4^+$ , and, therefore,  $\epsilon(\text{NO}_3^-)$  is close to 100% in group N in the two countries (Figure 14e). Besides, water uptake by hygroscopic aerosols increases the aerosol surface area and volume, enhancing the hydrolysis of  $\text{N}_2\text{O}_5$  across particles and forming  $\text{NO}_3^-$  (Tian et al., 2018; Wang et al., 2020b).

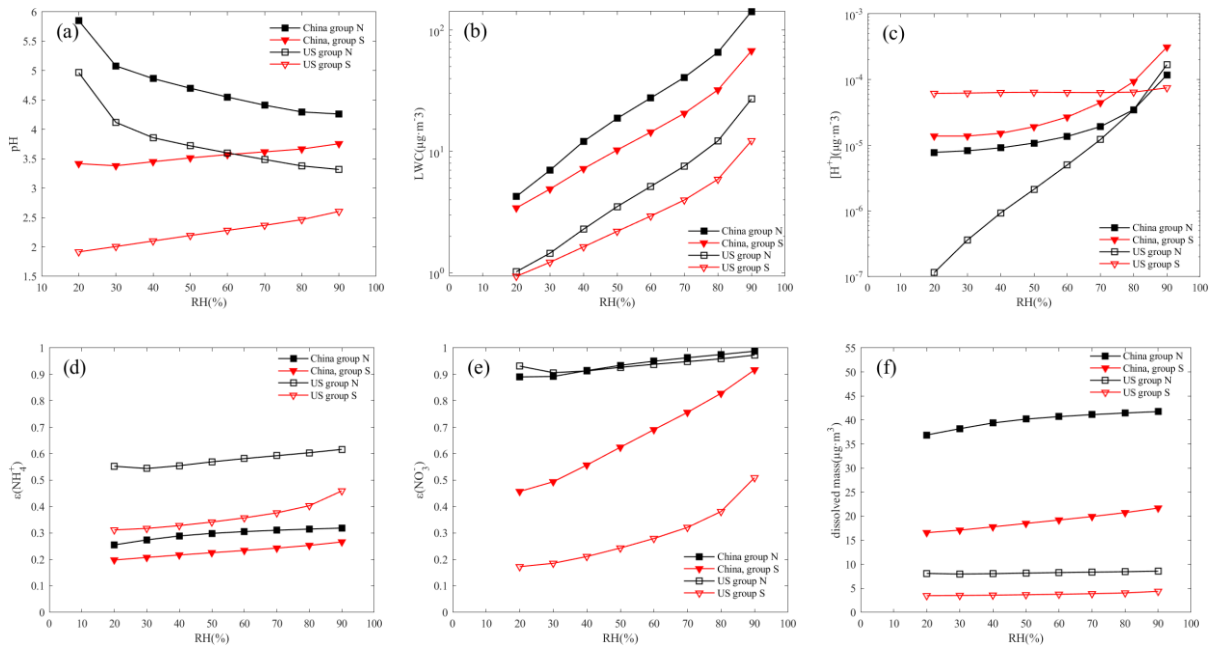


**Figure 14** Values of pH, LWC,  $\text{H}^+_{\text{air}}$ ,  $\epsilon(\text{NH}_4^+)$ ,  $\epsilon(\text{NO}_3^-)$  and dissolved mass in group N and group S under different RH conditions in China and the United States. China: group N, n=410; group S, n=470; US: group N, n=72; group S, n=1119.

The condition in group N usually has a higher LWC and aerosol mass, due to the mutual promotion between LWC and particle nitrate. And such a condition in group N occurs more often in China than in the US, which is probably one of the reasons leading to high particle concentrations on hazy days in China.

The nitrate/sulfate ratio depends on the emission ratio of  $\text{NO}_x/\text{SO}_2$ , the availability of cations due to the dependency of  $\epsilon(\text{NO}_3^-)$  on  $\text{TNH}_3$  (Figure 10c), and other factors such as the atmospheric oxidizing capacity. Further investigation into the total emissions shows that the emission molar ratios of  $[\text{NO}_x]/[\text{SO}_2]$  are close to 3:1 in both countries (2.92 in China in 2017 and 3.12 in the US in 2011 when assuming the emission  $\text{NO}_x$  is in the form of  $\text{NO}_2$ ), indicating that the emission difference is not the major factor leading to the nitrate/sulfate ratio difference. On the other hand, the emission molar ratio of  $[\text{NH}_3]/([\text{NO}_x]+2\times[\text{SO}_2])$  in China (0.75) is 1.6 times higher than that in the US (0.46), which is consistent with the measured high relative abundance of  $\text{TNH}_3$  in China and confirms that high availability of cations (mainly  $\text{NH}_4^+$  caused by high  $\text{NH}_3$  emission) is one of the causes for the high nitrate/sulfate ratio in China.

### 3.2.5 *Two pathways leading to the aerosol acidity difference.*

As aerosol pH is calculated as  $[\log_{10}(\text{LWC}) - \log_{10}(\text{H}_{\text{air}}^+) - 3]$ , all mechanisms affecting aerosol pH must be through the modification of LWC,  $\text{H}_{\text{air}}^+$ , or both (LWC and  $\text{H}_{\text{air}}^+$  are expressed as mass per unit volume of air,  $\mu\text{g m}^{-3}$ ). We quantitatively separate the contributions of individual factors to the China-US pH difference into the LWC-modifying pathway and the  $\text{H}_{\text{air}}^+$ -modifying pathway (Figure 9). To achieve this, we use MTSM to quantify the contributions of individual factors to the differences in  $\log_{10}(\text{LWC})$  and  $[-\log_{10}(\text{H}_{\text{air}}^+)-3]$ , respectively, between the two countries, with the same approach as we did for pH (LWC and  $\text{H}_{\text{air}}^+$  are two output variables directly predicted by ISORROPIA). The results show that both the changes in LWC and  $\text{H}_{\text{air}}^+$  lead to increases in aerosol pH when conditions change from those in the US to China.

Given that LWC increases with aerosol mass concentration (Song et al., 2019), higher component concentrations in China than in the US increase LWC and, thus, increase aerosol pH (Figure 9b). Through the LWC-modifying pathway, changes in  $\text{SO}_4$ ,  $\text{TNH}_3$ , and  $\text{TNO}_3$  lead to increases in pH (0.15–0.3) (Figure 9b), which are consistent in all three groups. Compared to other groups, the observation group represents a higher pH increase due to Cl and a higher pH decrease due to RH (Figure 9b), mainly because of the larger differences in Cl concentrations and RH for this group than for other groups (Table 3).

Through the  $\text{H}_{\text{air}}^+$ -modifying pathway, the effects of individual factors on pH changes vary (Figure 9c). Increases in acidic components ( $\text{SO}_4$  and  $\text{TNO}_3$ ) increase  $\text{H}_{\text{air}}^+$  and thus decrease aerosol pH (Figure 9c). Increases in  $\text{TNH}_3$ , TCl, and NVCs, on the other hand, decrease  $\text{H}_{\text{air}}^+$  and increase aerosol pH (Figure 9c). By increasing  $\text{H}_{\text{air}}^+$ , increased  $\text{SO}_4$  decreases pH by 0.7–1.2 units, showing a much stronger acidic capacity than another acidic component,  $\text{TNO}_3$ , which only decreases pH by 0.17–0.27 units (Figure 9c). Compared to the US, China is in a  $\text{TNH}_3$ -rich condition. The molar ratios of  $[\text{TNH}_3] / (2 \times [\text{SO}_4] + [\text{TNO}_3] + [\text{TCl}])$  in China vs. in the US are 3 vs. 1.4, 2.0 vs. 1.0, and 2.4 vs. 1.5 in the observation, non-weighted, and population-weighted groups, respectively. Changing the conditions from the US to China,  $\text{TNH}_3$  plays the most important role in neutralizing the acidic components and driving the pH increase in the  $\text{H}_{\text{air}}^+$ -modifying pathway (Figure 9c).

For individual factors, the net changes in pH are a result of the combination of the two pathways. For example, increased  $\text{SO}_4$  increases LWC and  $\text{H}_{\text{air}}^+$  simultaneously. The increase in LWC increases aerosol pH, while the increase in  $\text{H}_{\text{air}}^+$  decreases aerosol pH. All three groups suggest that the effect of  $\text{H}_{\text{air}}^+$  on pH overwhelms that of LWC on pH,

leading to a net decrease in pH from an  $\text{SO}_4$  increase (Figure 9). Increased  $\text{TNH}_3$  increases pH in both pathways, adding up to a larger increase in pH (Figure 9). Increased  $\text{TNO}_3$  through these two pathways, however, is associated with opposite effects on pH which are comparable in magnitude and thus tends to offset each other (especially in the observation group) (Figure 9). This explains the aforementioned small change in pH from the  $\text{TNO}_3$  increases. Combining all the factors, both pathways increase aerosol pH, resulting in the large difference in aerosol acidity between these two countries.

To facilitate a follow-up sensitivity test to link the two pathways with mass concentration and chemical composition, we define the total mass concentration as the sum of the mass concentrations of all the eight input components (i.e.,  $\text{Na}^+$ ,  $\text{SO}_4$ ,  $\text{TNH}_3$ ,  $\text{TNO}_3$ ,  $\text{TCl}$ ,  $\text{Ca}^{2+}$ ,  $\text{K}^+$ , and  $\text{Mg}^{2+}$ ), including both gas and particle phases, and the chemical composition as the composition of the eight components in the aerosol (gas + particle) system. The observation pH group shows that the total mass concentration in China is 8.4 times that in the US, and the chemical composition in China is richer in  $\text{TNH}_3$  than that in the US (as illustrated by the ratios of  $[\text{TNH}_3] / (2 \times [\text{SO}_4] + [\text{TNO}_3] + [\text{TCl}])$  mentioned above). It has been found that both LWC and  $\text{H}_{\text{air}}^+$  are affected by mass concentration and aerosol composition (Guo et al., 2015; Xie et al., 2019; Zheng et al., 2020). To investigate how the differences in mass concentration and composition between China and the US is associated with the LWC- and  $\text{H}_{\text{air}}^+$ -modifying pathways and consequently the pH difference, we first increase the mass concentrations of individual input components in the US case by a constant factor of 8.4, whereby we get an intervening case representing the overall pollution level as in China but with the chemical composition feature as in the US (Table 3, sensitivity test). From the intervening case, we then shift the composition of

the US case to that of China (Table 3, sensitivity test). Note that throughout this sensitivity test, meteorological conditions are held constant. The results are shown in Figure 15. The first step by increasing the mass concentration yields an increase of 1.02 units in the aerosol pH which is mainly achieved through the LWC-modifying pathway (1.06 units) instead of the  $H_{air}^+$ -modifying pathway (-0.04 unit) (Figure 15 (a), (b), (c)). The second step by changing the chemical composition shows a further increase of 0.76 units in the aerosol pH which is mainly achieved through the  $H_{air}^+$ -modifying pathway (0.88 units), whereas the LWC-modifying pathway (-0.11 unit) plays a minor role (Figure 15 (d), (e), (f)). This sensitivity test reveals that the LWC-modifying pathway is mainly associated with the change in mass concentration, and the  $H_{air}^+$ -modifying pathway is mainly associated with the change in chemical composition.

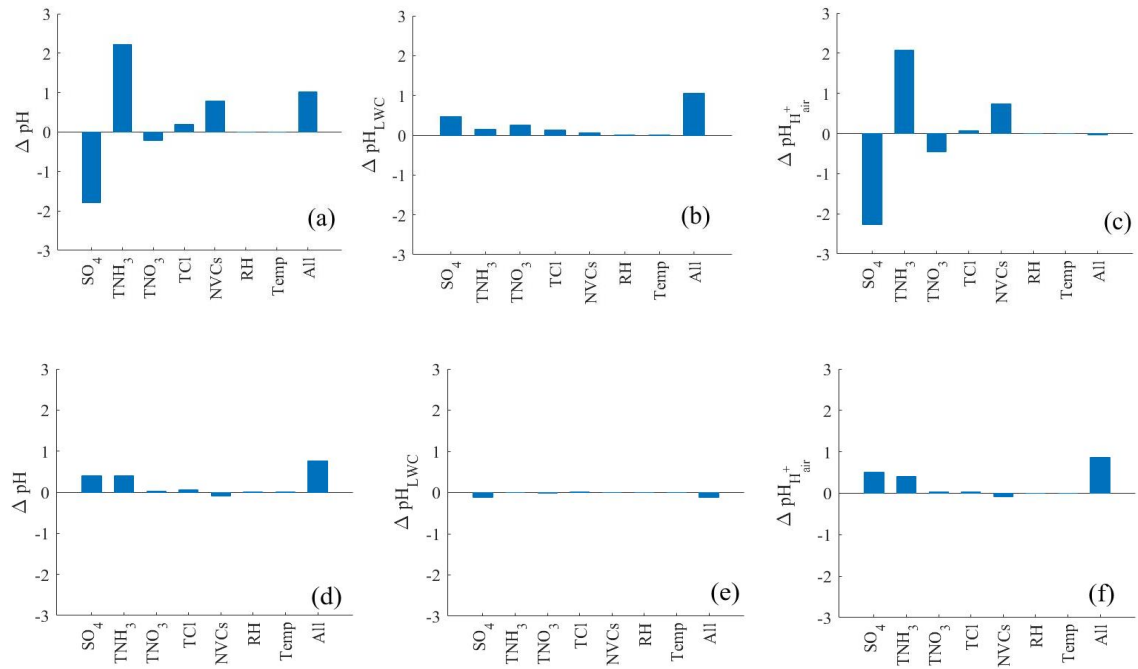


**Figure 15 Step-specific contributions of individual factors to the pH difference between China and the US. (a), (b), and (c) show the contributions of individual components and meteorological factors to (a) total difference of aerosol pH ( $\Delta pH$ ), (b) through the pathway of LWC ( $\Delta pH_{LWC}$ ), (c) through the pathway of  $H^+$ air**

$(\Delta pH_{H^+_{air}})$  between the US case and an intervening case with the concentrations of all components in the US case multiplied by a constant factor of 8.4. The former is chosen as the starting point, and the latter is chosen as the ending point. (d), (e), and (f) show the contributions of individual components and meteorological factors to (d) total difference of aerosol pH ( $\Delta pH$ ), (e) through the pathway of LWC ( $\Delta pH_{LWC}$ ), (f) through the pathway of  $H^+_{air}$  ( $\Delta pH_{H^+_{air}}$ ) between the intervening case and the China case. The former is chosen as the starting point, and the latter is chosen as the ending point. The inputs are shown in Table 3, sensitivity test.

The increased pH in the first step is surprising as we initially thought that the pH should be unchanged before and after multiplying the concentration of each component with a constant factor. Further investigation shows that, during the first step, increased aerosol concentration drives more fractions of  $TNO_3$  and  $TNH_3$  partitioning into particle phases— $\epsilon(NH_4^+)$  and  $\epsilon(NO_3^-)$  increase from 0.4 and 0.6 to 0.6 and 0.98, respectively. Therefore, although the chemical composition of the aerosol system keeps constant, the particle composition changes. This repartitioning can be explained by the Henry's Law,  $[A_{aq}] = H_A \cdot p_A$ , where  $[A_{aq}]$  is the aqueous-phase concentration of A in the unit of moles per liter water,  $p_A$  is the partial pressure of A in the gas phase, and  $H_A$  is the Henry's law coefficient (Seinfeld and Pandis, 2006). In the first step after multiplying the constant factor, assuming no repartitioning,  $p_A$  increases due to the increased concentration of A in the gas phase, while  $[A_{aq}]$  remains largely constant because of the simultaneous increases in LWC and particle-phase A concentration ( $c_A$ ), given that  $[A_{aq}]$  is proportional to  $c_A \cdot LWC^{-1}$  (note that LWC and  $c_A$  are expressed as mass per unit volume of air, and  $[A_{aq}]$  is expressed as moles per unit volume of water). According to the Henry's Law, more gas-phase A will dissolve in water, and thus, the total A in the system shift toward the particle phase after the multiplication of the constant factor. Due likely to the weak acidic capacity of  $NO_3^-$  which is overwhelmed by  $NH_4^+$ , the particle is ultimately neutralized by the increased  $NH_4^+$  in the first step.

We find that by increasing the concentration of every component by a constant factor, the magnitude and direction of the resulting change in pH are sensitive to the fraction of  $\text{TNH}_3$  in the aerosol system while insensitive to the ratio of  $\text{SO}_4$  to  $\text{TNO}_3$ . Based on an  $\text{NH}_4^+ \text{-SO}_4^{2-} \text{-NO}_3^- \text{-H}_2\text{O}$  system, we conduct a series of sensitive tests to investigate the change in aerosol pH in response to the multiplication of a constant factor of 8.4 (Figure 16). The change in pH reduces gradually from 1.2 units to 0.8 unit when the  $\text{TNH}_3$  mass fraction of the system decreases from 67% to 27%. With further decreases in the  $\text{TNH}_3$  fraction, the increase in pH diminishes rapidly, becomes negative when the  $\text{TNH}_3$  mass fraction is lower than 25%, and is -0.6 when the  $\text{TNH}_3$  mass fraction is 17%. Under a constant  $\text{TNH}_3$  mass fraction, the change in pH remain generally constant across a wide range of the mass ratios of  $\text{SO}_4$  to  $\text{TNO}_3$  (from 5:1 to 1:5). In populated continental regions, mass fractions of  $\text{TNH}_3$  are often found high (Bencs et al., 2008; Behera and Sharma, 2010; Zheng et al., 2015; Cheng et al., 2016; Guo et al., 2017b), and the pH increase rather than decrease in response to the multiplication is thus expected.

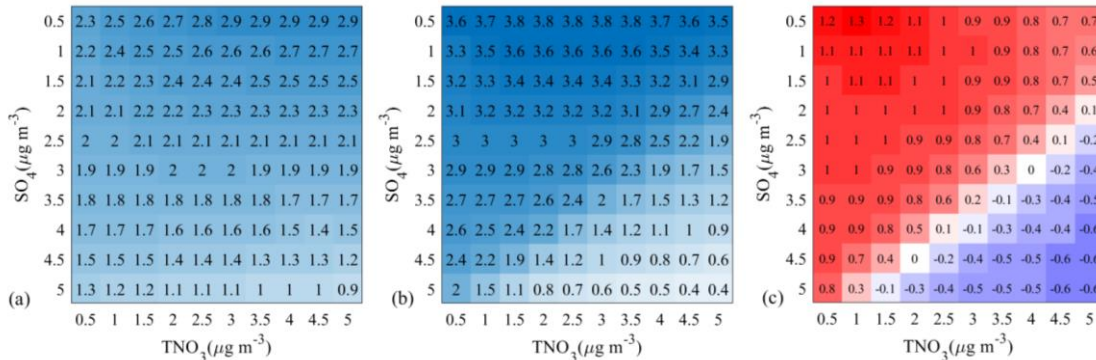


**Figure 16. Sensitivity tests showing the pH changes in response to different levels of  $\text{SO}_4$  and  $\text{TNO}_3$  in an  $\text{NH}_4^+ \text{-SO}_4^{2-} \text{-NO}_3^- \text{-H}_2\text{O}$  system. (a) The pH of an aerosol with fixed  $\text{TNH}_3$  ( $2 \mu\text{g m}^{-3}$ ) and varied  $\text{SO}_4$  and  $\text{TNO}_3$  (from  $0.5 \mu\text{g m}^{-3}$  to  $5 \mu\text{g m}^{-3}$ ) (b) The pH after multiplying all the inputs in (a) by a factor of 8.4. Note that the  $\text{SO}_4$  and**

**TNO<sub>3</sub> levels shown along the axes are the initial levels before multiplication. (c) pH differences between (b) and (a) (b minus a).**

Such an assessment by tracking pathway- and step-specific contributions provides a better understanding of the pH difference between China and the US. We show that through the LWC-modifying pathway, the increases in aerosol components consistently lead to increases in pH, and that through the H<sub>air</sub><sup>+</sup>-modifying pathway, the effects of different components on pH vary in direction. If the LWC-modifying pathway dominated the pH changes over the H<sub>air</sub><sup>+</sup>-modifying pathway, aerosol mass concentrations would be the main factor driving the aerosol acidity difference between China and the US, and one could simply attribute the difference in aerosol acidity to the fact that China is more polluted than the US. In contrast, if the H<sub>air</sub><sup>+</sup>-modifying pathway dominated, chemical composition would be the dominant factor, and the compound profiles of precursors emissions, which affect the availability of the corresponding aerosol components in the air, would play an important role. While there has been debate about whether mass concentration or chemical composition plays a more important role in determining aerosol pH (Cheng et al., 2016;Guo et al., 2017a;Pye et al., 2020;Zheng et al., 2020), our results suggest that both are important in explaining the China-US pH difference (Figure 9). The three groups are not consistent with each other in which pathway contributes more than the other to the pH difference, but they all suggest that the two pathways are comparable in terms of their effects on aerosol pH (Figure 9b and c).

Our results, showing the importance of both mass concentration associated with LWC and chemical composition associated with H<sub>air</sub><sup>+</sup> and a minor role of temperature, seem in some aspects to contradict a previous study (Zheng et al., 2020) which highlighted LWC

and temperature instead of chemical composition as the most important factors explaining the pH difference between China (NCP) and the US. We note that the difference in the conclusions is reasonable when considering the differences in the specific cases examined in these two studies. The previous study compared the conditions in NCP in winter with those in the southeastern US in summer (SE-US). Because of the differences in latitude (north for China vs south for the US) and season (winter for China vs summer for the US), the difference in temperature between their scenarios (29 K) was an order of magnitude greater than those in our study which has greater spatial and temporal coverage (2.6 K in the observation group, 5 K in the non-weighted group, and -1.4 K in the population-weighted group). Using MTSM, we evaluate the pH difference between NCP and SE-US scenarios considered in the previous study. The results show that temperature accounts for 1.3 units of difference in aerosol pH between their two scenarios (Figure 17), in line with what was previously reported (1.6 units).

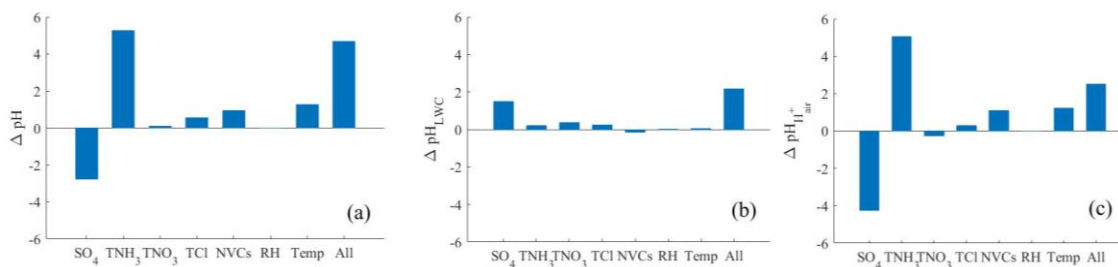


**Figure 17 Contributions of individual components and meteorological factors to (a) total difference of aerosol pH ( $\Delta pH$ ), (b) through the pathway of LWC ( $\Delta pH_{LWC}$ ), (c) through the pathway of H+air ( $\Delta pH_{H+air}$ ) calculated by Multivariable Taylor Series Method (MTSM) between the NCP scenario and the US-SE scenario in Zheng's study (Zheng et al., 2020). For individual factors, the sum of the contributions through the two pathways yields the net contribution of this factor to aerosol pH. The case in the United States is chosen as the starting point, and China as the ending point.**

In addition, ISORROPIA simulations show a LWC difference of  $8.2 \mu\text{g}\cdot\text{m}^{-3}$  between China (NCP) and the contiguous US in the “observation” group in our study and  $340 \mu\text{g}\cdot\text{m}^{-3}$  between the scenarios considered in the previous study. The much larger LWC difference in the previous study compared to ours is mainly driven by the differences in pollutant concentrations. For example, the  $\text{SO}_4$  concentration is as high as  $156 \mu\text{g}\cdot\text{m}^{-3}$  in the NCP scenario in the previous study but only  $9.2 \mu\text{g}\cdot\text{m}^{-3}$  in our study. Such differences in concentrations are reasonable, given that the previous study selected a severe haze event occurring in Beijing in winter 2013 as the scenario for China (NCP), while we use annual average levels over NCP in 2017 as our case for China (NCP). Note that winter 2013 was a period when air pollution reportedly reached record high levels across northern China (Wang et al., 2014b; Li et al., 2016). Since 2013, China has launched strict controls on air pollutant emissions, and  $\text{PM}_{2.5}$  levels have decreased significantly between 2013 and 2017 (Zhang et al., 2019). Therefore, the NCP scenario in the previous study should be more representative of short-term haze events in the pre-2013 period, while our China (NCP) case should be more representative of annual average levels in recent years.

## CHAPTER 4. CONCLUSIONS AND IMPLICATIONS

Based on extended ground-level measurements and regional air quality model simulations, we find significant differences in aerosol pH between China and the US. Aerosols in the US are on average more acidic with pH generally 1–2 units lower than in China. We propose an MTSM method to identify the key factors leading to the pH difference. The MTSM analysis reveals the important role of  $\text{TNH}_3$  in causing the pH difference and an opposing effect from  $\text{SO}_4$  which partially offsets the positive effect of  $\text{TNH}_3$  on the pH change. Other factors play relatively minor roles. Further investigation highlights two pathways, one associated with changes in LWC and the other with changes in  $\text{H}_{\text{air}}^+$ , linking to the pH difference. The increased mass concentration in China, compared to the US, enhances LWC, and the change in chemical composition toward a  $\text{TNH}_3$ -rich condition reduces  $\text{H}_{\text{air}}^+$ . Both pathways facilitate the increases in aerosol pH in China and are comparable in terms of driving the pH increase.

While in this study we used MTSM to quantify the contributions of each factors to aerosol pH difference under the annual average conditions, we believe our method could have more widely use. It can be used to exploring the driving force in other locations as well as in different timeframe. For example, our results showed that temperature has a minor effect on causing aerosol pH difference, but the effect of temperature will stand out if we study two cases with different season. And it might be a potential important effect in causing seasonal variation.

Previous studies have suggested that low aerosol pH is associated with increased toxicity because of the increased solubility of transition metals in aerosol LWC, which induce

airway injury and inflammation through the production of reactive oxygen species in vivo (Kim et al., 2015). The lower aerosol pH in the US than in China implies that aerosols in the US may be more toxic than in China. However, this implication should be interpreted with caution because there are other known pathways through which particulate matter can harm humans, and the mechanisms of how particulate matter affects health are not completely understood (Armstrong et al., 2004). More studies are needed to assess the health outcomes associated with the disparity in aerosol pH between the two countries.

# APPENDIX A. INFORMATION OF MONITORING SITES USED IN THIS STUDY

## A.1 Information of monitoring sites in the US

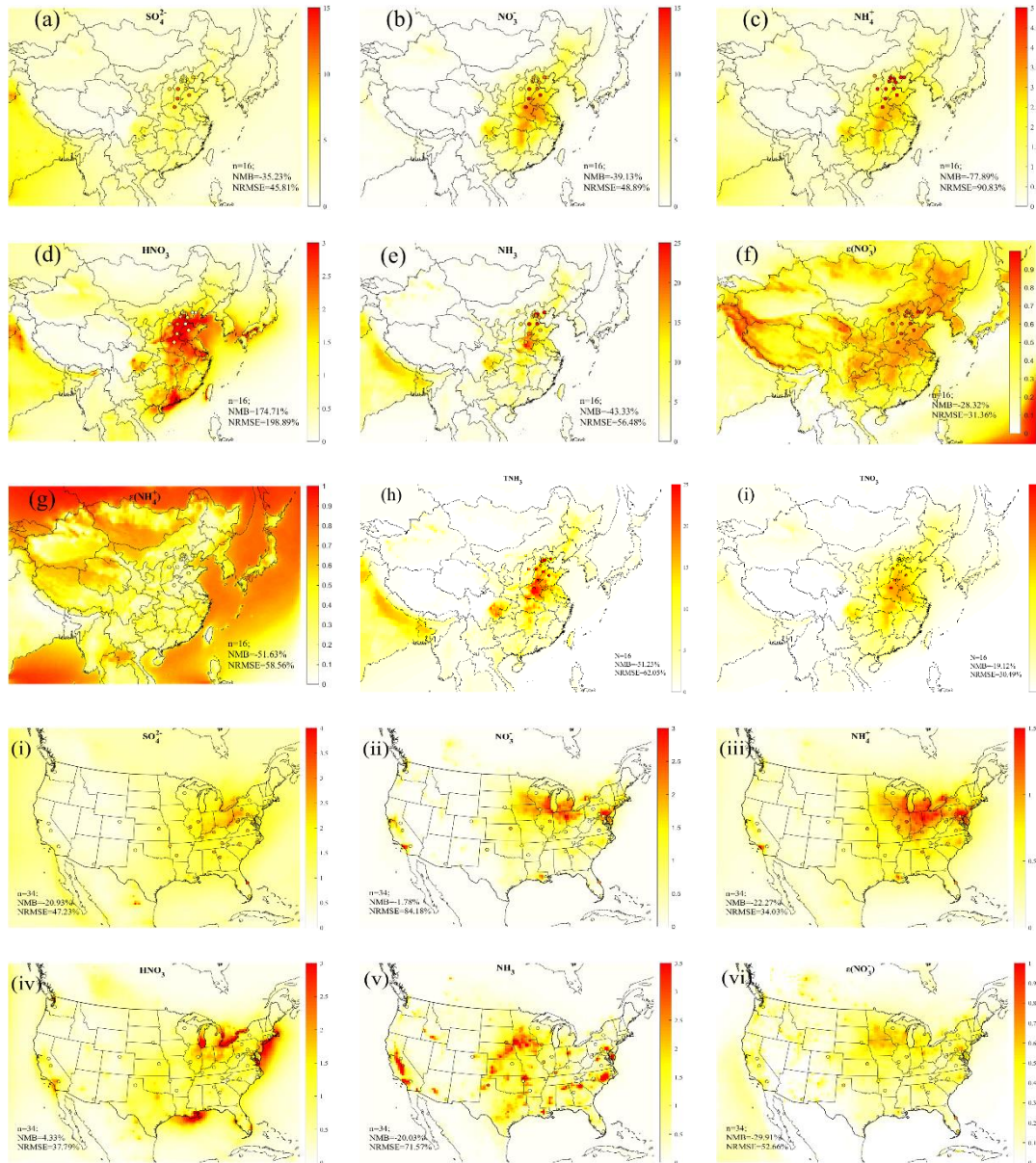
No.	Site name	Latitude	Longitude
1	Parsons	39.09	-79.66
2	Prince Edward	37.17	-78.31
3	Perkiinstown	45.21	-90.60
4	Rocky Mtn NP Collocated	40.28	-105.55
5	Sand Mountain	34.29	-85.97
6	Stockton	42.29	-90.00
7	Sequoia NP - Ash Mountain	36.49	-118.83
8	Wash. Crossing	40.31	-74.87
9	Yosemite NP - Turtleback Dome	37.71	-119.71
10	Abington	41.84	-72.01
11	Alhambra	38.87	-89.62
12	Arendtsville	39.92	-77.31
13	Beaufort	34.88	-76.62
14	Caddo Valley	34.18	-93.10
15	Cadiz	36.78	-87.85
16	Chiricahua NM	32.01	-109.39
17	Cherokee Nation	35.75	-94.67
18	Candor	35.26	-79.84
19	Coweeta	35.06	-83.43
20	Connecticut Hill	42.40	-76.65
21	Deer Creek	39.64	-83.26
22	Georgia Station	33.18	-84.41
23	Palo Duro	34.88	-101.67
24	Joshua Tree NP	34.07	-116.39
25	Bondville	40.05	-88.37
26	Great Smoky NP - Look Rock	35.63	-83.94
27	Indian River Lagoon	27.85	-80.46
28	Santee Sioux	42.83	-97.85
29	Beltsville	39.03	-76.82
30	Everglades NP	25.39	-80.68
31	Mount Rainier NP	46.76	-122.12
32	Kane Exp. Forest	41.60	-78.77
33	Konza Prairie	39.10	-96.61
34	Mackville	37.70	-85.05

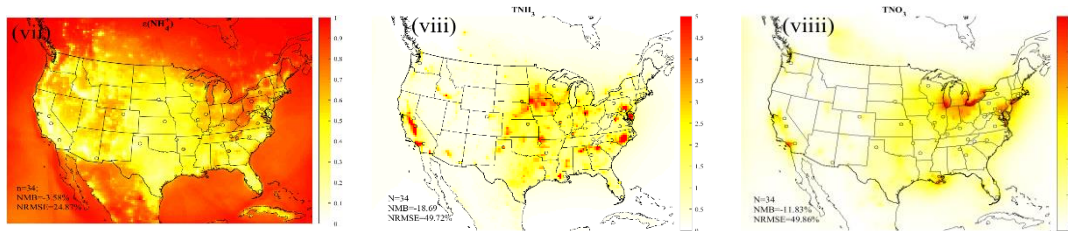
## A.2 Information of monitoring sites in China

No.	Site name	Latitude	Longitude
1	Chinese Research Academy of Environmental Science (CRAES)	40.04	116.42
2	Anyang	36.09	114.39
3	Baoding	38.87	115.52
4	Dezhou	37.45	116.32
5	Hohhot	40.80	111.64
6	Jinan	36.66	117.05
7	Liulihe	39.58	116.00
8	Qinhuangdao	39.91	119.56
9	Shijiazhuang	38.03	114.54
10	Taiyuan	37.82	112.57
11	Tangshang	39.90	118.60
12	Tianjin	39.10	117.17
13	Xianghe	39.78	116.96
14	Yizhuang	39.80	116.51
15	Yufa	39.52	116.31
16	Zhengzhou	34.28	113.68

# APPENDIX B. MODEL EVALUATION RESULTS

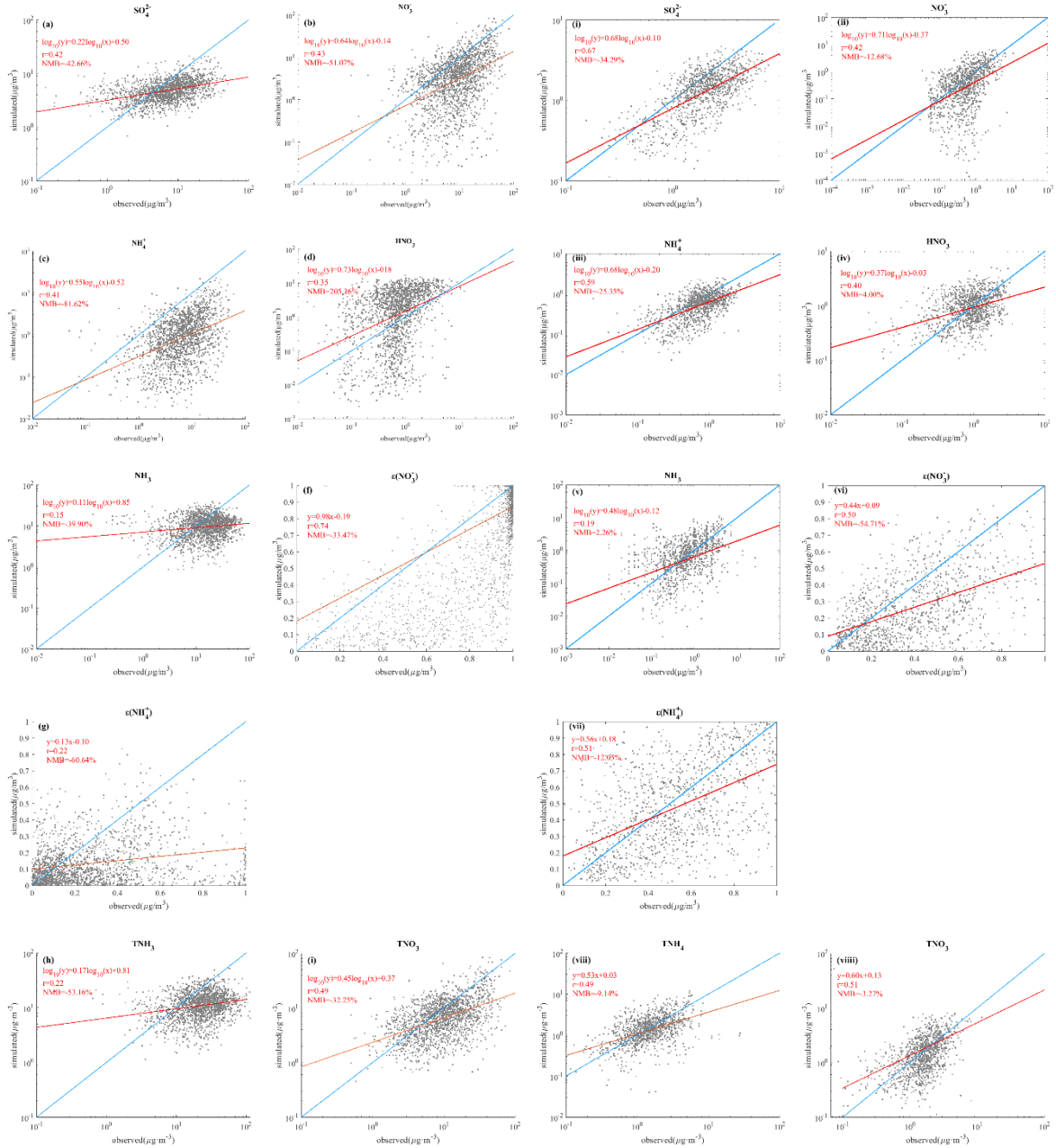
## B.1 Annual mean concentrations of gaseous and aerosol species





**Figure B1 Annual mean concentrations of  $\text{PM}_{2.5}$  components  $\text{SO}_4^{2-}$ ,  $\text{NO}_3^-$ ,  $\text{NH}_4^+$ , gaseous components  $\text{HNO}_3$  and  $\text{NH}_3$  and the partitioning including  $\varepsilon(\text{NO}_3^-)$  and  $\varepsilon(\text{NH}_4^+)$  based on CMAQ simulations (colored map) and observations (colored dots) in China (panels a-g) and in the United States (panels i-vii). Normalized mean bias (NMB) and normalized root mean square error (NRMSE) are shown on each panel.**

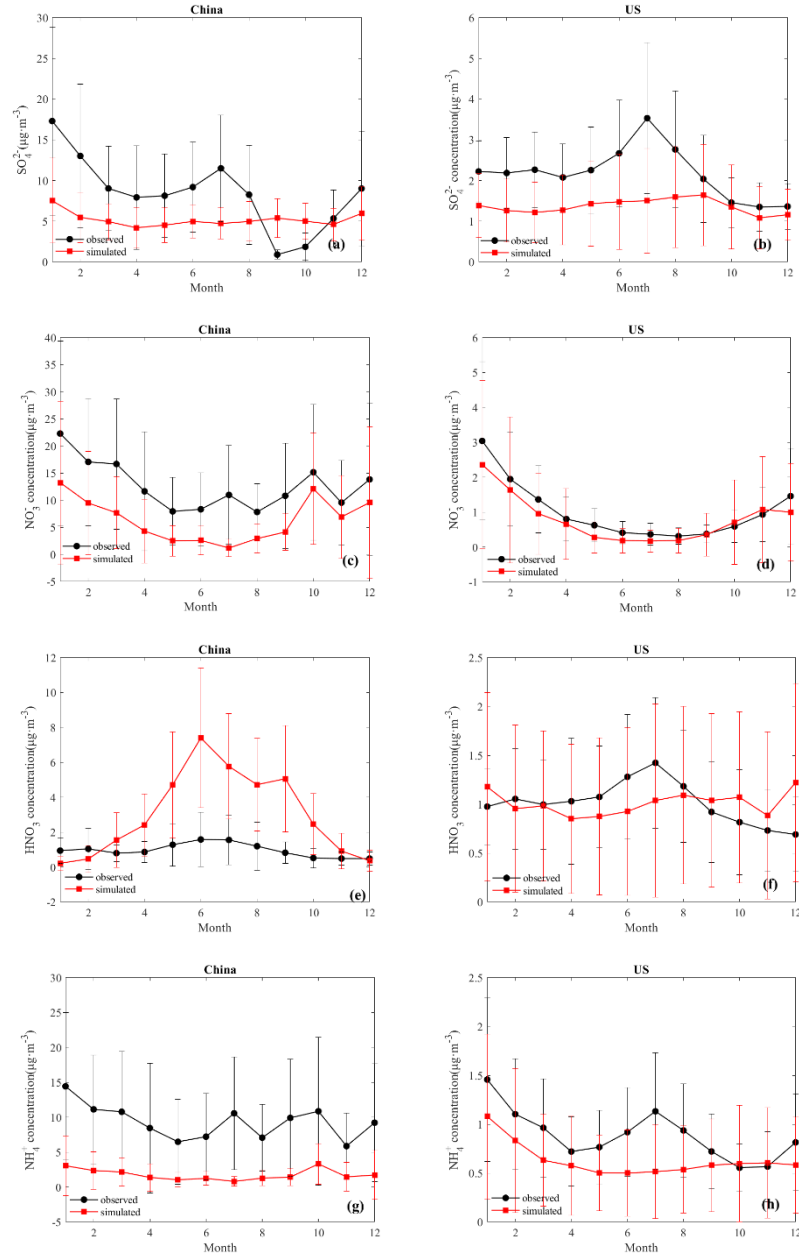
## B.2 Scatter plots of observed values versus simulated values of gaseous and aerosol species.



**Figure B2** Comparison of daily observed and CMAQ simulated aerosol component concentrations of  $\text{SO}_4^{2-}$ ,  $\text{NO}_3^-$ ,  $\text{NH}_4^+$ , gaseous concentrations of  $\text{HNO}_3$  and  $\text{NH}_3$  and the partitioning  $\epsilon(\text{NO}_3^-)$  and  $\epsilon(\text{NH}_4^+)$  in China (panels a-g) and in the United States (panels i-vii).

**The regression line (red), 1:1 line (blue), regression equation and correlation coefficient  $r$  are shown in each panel.**

### B.3 Monthly trend of gaseous and aerosol species based on observed values and simulated values.



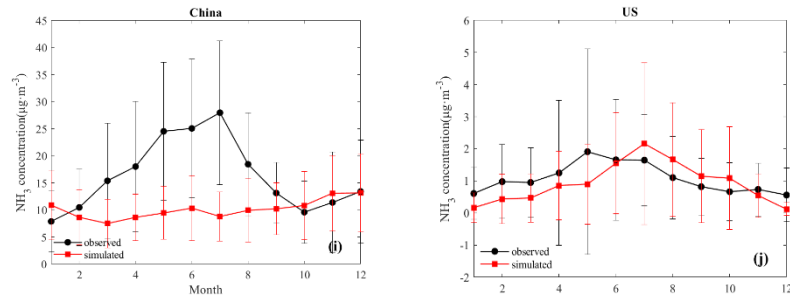


**Figure B3 Monthly average concentrations of  $\text{SO}_4^{2-}$ ,  $\text{NO}_3^-$ ,  $\text{HNO}_3^-$ ,  $\text{NH}_4^+$ ,  $\text{NH}_3$  : observed versus CMAQ simulated data in China (panels a, c, e, g, i) and in the United States (panels b, d, f, h, j). The error bars represent the standard deviation of all the cases in each month.**

## REFERENCES

- AiMa Air Quality Forecasting System: [http://www.aimayubao.com/wryb\\_eval.php?movie=no](http://www.aimayubao.com/wryb_eval.php?movie=no), 2017.
- Armstrong, B., Hutchinson, E., Unwin, J., and Fletcher, T.: Lung cancer risk after exposure to polycyclic aromatic hydrocarbons: a review and meta-analysis, *Environ Health Perspect*, 112, 970-978, 10.1289/ehp.6895, 2004.
- Battaglia, M. A., Douglas, S., and Hennigan, C. J.: Effect of the Urban Heat Island on Aerosol pH, *Environ Sci Technol*, 51, 13095-13103, 10.1021/acs.est.7b02786, 2017.
- Behera, S. N., and Sharma, M.: Investigating the potential role of ammonia in ion chemistry of fine particulate matter formation for an urban environment, *Science of The Total Environment*, 408, 3569-3575, <https://doi.org/10.1016/j.scitotenv.2010.04.017>, 2010.
- Behera, S. N., Betha, R., and Balasubramanian, R.: Insights into Chemical Coupling among Acidic Gases, Ammonia and Secondary Inorganic Aerosols, *Aerosol and Air Quality Research*, 13, 1282-1296, 10.4209/aaqr.2012.11.0328, 2013.
- Behera, S. N., Cheng, J., Huang, X., Zhu, Q., Liu, P., and Balasubramanian, R.: Chemical composition and acidity of size-fractionated inorganic aerosols of 2013-14 winter haze in Shanghai and associated health risk of toxic elements, *Atmospheric Environment*, 122, 259-271, <https://doi.org/10.1016/j.atmosenv.2015.09.053>, 2015.
- Bencs, L., Khaiwal, R., Hoog, J., Rasoazanany, E., Deutsch, F., Bleux, N., Berghmans, P., Roekens, E., Krata, A., and Van Grieken, R.: Mass and ionic composition of atmospheric fine particles over Belgium and their relation with gaseous air pollutants, *Journal of Environmental Monitoring*, 10, 1148-1157, 10.1039/B805157G, 2008.
- Burnett, R. T., Pope, C. A., 3rd, Ezzati, M., Olives, C., Lim, S. S., Mehta, S., Shin, H. H., Singh, G., Hubbell, B., Brauer, M., Anderson, H. R., Smith, K. R., Balmes, J. R., Bruce, N. G., Kan, H., Laden, F., Prüss-Ustün, A., Turner, M. C., Gapstur, S. M., Diver, W. R., and Cohen, A.: An integrated risk function for estimating the global burden of disease attributable to ambient fine particulate matter exposure, *Environ Health Perspect*, 122, 397-403, 10.1289/ehp.1307049, 2014.
- Butler, T., Vermeylen, F., Lehmann, C. M., Likens, G. E., and Puchalski, M.: Increasing ammonia concentration trends in large regions of the USA derived from the NADP/AMoN network, *Atmospheric Environment*, 146, 132-140, <https://doi.org/10.1016/j.atmosenv.2016.06.033>, 2016.
- Chen, Y. L., Shen, H. Z., and Russell, A. G.: Current and Future Responses of Aerosol pH and Composition in the US to Declining SO<sub>2</sub> Emissions and Increasing NH<sub>3</sub> Emissions, *Environ Sci Technol*, 53, 9646-9655, 10.1021/acs.est.9b02005, 2019.

Cheng, Y., Zheng, G., Wei, C., Mu, Q., Zheng, B., Wang, Z., Gao, M., Zhang, Q., He, K., Carmichael, G., Pöschl, U., and Su, H.: Reactive nitrogen chemistry in aerosol water as a source of sulfate during haze events in China, *Science Advances*, 2, e1601530, 10.1126/sciadv.1601530, 2016.

Clegg, S. L., Brimblecombe, P., and Wexler, A. S.: Thermodynamic Model of the System  $\text{H}^+ - \text{NH}_4^+ - \text{SO}_4^{2-} - \text{NO}_3^- - \text{H}_2\text{O}$  at Tropospheric Temperatures, *The Journal of Physical Chemistry A*, 102, 2137-2154, 10.1021/jp973042r, 1998.

Cui, Y., Yin, Y., Chen, K., Zhang, X., Kuang, X., Jiang, H., Wang, H., Zhen, Z., and He, C.: Characteristics and sources of WSI in North China Plain: A simultaneous measurement at the summit and foot of Mount Tai, *Journal of Environmental Sciences*, 92, 264-277, <https://doi.org/10.1016/j.jes.2020.02.017>, 2020.

Ding, J., Zhao, P., Su, J., Dong, Q., Du, X., and Zhang, Y.: Aerosol pH and its driving factors in Beijing, *Atmos. Chem. Phys.*, 19, 7939-7954, 10.5194/acp-19-7939-2019, 2019.

Fang, T., Guo, H., Verma, V., Peltier, R. E., and Weber, R. J.: PM<sub>2.5</sub> water-soluble elements in the southeastern United States: automated analytical method development, spatiotemporal distributions, source apportionment, and implications for health studies, *Atmos. Chem. Phys.*, 15, 11667-11682, 10.5194/acp-15-11667-2015, 2015.

Fang, T., Guo, H., Zeng, L., Verma, V., Nenes, A., and Weber, R. J.: Highly Acidic Ambient Particles, Soluble Metals, and Oxidative Potential: A Link between Sulfate and Aerosol Toxicity, *Environ Sci Technol*, 51, 2611-2620, 10.1021/acs.est.6b06151, 2017.

Feng, J., Chan, E., and Vet, R.: Air quality in the eastern United States and Eastern Canada for 1990–2015: 25 years of change in response to emission reductions of SO<sub>2</sub> and NO<sub>x</sub> in the region, *Atmos. Chem. Phys.*, 20, 3107-3134, 10.5194/acp-20-3107-2020, 2020.

Fountoukis, C., and Nenes, A.: ISORROPIA II: a computationally efficient thermodynamic equilibrium model for  $\text{K}^+ - \text{Ca}^{2+} - \text{Mg}^{2+} - \text{NH}_4^+ - \text{Na}^+ - \text{SO}_4^{2-} - \text{NO}_3^- - \text{Cl}^- - \text{H}_2\text{O}$  aerosols, *Atmos. Chem. Phys.*, 7, 4639-4659, 10.5194/acp-7-4639-2007, 2007.

Fountoukis, C., Koraj, D., Van Der Gon, H. D., Charalampidis, P., Pilinis, C., and Pandis, S.: Impact of grid resolution on the predicted fine PM by a regional 3-D chemical transport model, *Atmos. Environ.*, 68, 24-32, 2013.

Freedman, M. A., Ott, E.-J. E., and Marak, K. E.: Role of pH in Aerosol Processes and Measurement Challenges, *The Journal of Physical Chemistry A*, 123, 1275-1284, 10.1021/acs.jpca.8b10676, 2019.

Ge, B., Xu, X., Ma, Z., Pan, X., Wang, Z., Lin, W., Ouyang, B., Xu, D., Lee, J., Zheng, M., Ji, D., Sun, Y., Dong, H., Squires, F. A., Fu, P., and Wang, Z.: Role of Ammonia on the Feedback Between AWC and Inorganic Aerosol Formation During Heavy Pollution in the North China Plain, *Earth and Space Science*, 6, 1675-1693, 10.1029/2019EA000799, 2019.

Ge, Z., Wexler, A. S., and Johnston, M. V.: Deliquescence Behavior of Multicomponent Aerosols, *The Journal of Physical Chemistry A*, 102, 173-180, 10.1021/jp972396f, 1998.

NCEP Product Inventory - Global Products:  
<https://www.nco.ncep.noaa.gov/pmb/products/gfs/#GFS>.

Guo, H., Xu, L., Bougiatioti, A., Cerully, K. M., Capps, S. L., Hite Jr, J. R., Carlton, A. G., Lee, S. H., Bergin, M. H., Ng, N. L., Nenes, A., and Weber, R. J.: Fine-particle water and pH in the southeastern United States, *Atmos. Chem. Phys.*, 15, 5211-5228, 10.5194/acp-15-5211-2015, 2015.

Guo, H., Sullivan, A. P., Campuzano-Jost, P., Schroder, J. C., Lopez-Hilfiker, F. D., Dibb, J. E., Jimenez, J. L., Thornton, J. A., Brown, S. S., Nenes, A., and Weber, R. J.: Fine particle pH and the partitioning of nitric acid during winter in the northeastern United States, *Journal of Geophysical Research: Atmospheres*, 121, 10,355-310,376, 10.1002/2016jd025311, 2016.

Guo, H., Liu, J., Froyd, K., Robert, J., Veres, P., Hayes, P., Jimenez, J., Nenes, A., and Weber, R.: Fine particle pH and gas-particle phase partitioning of inorganic species in Pasadena, California, during the 2010 CalNex campaign, *Atmospheric Chemistry and Physics Discussions*, 1-33, 10.5194/acp-2016-1158, 2017a.

Guo, H., Weber, R. J., and Nenes, A.: High levels of ammonia do not raise fine particle pH sufficiently to yield nitrogen oxide-dominated sulfate production, *Scientific Reports*, 7, 12109, 10.1038/s41598-017-11704-0, 2017b.

Guo, H., Otjes, R., Schlag, P., Kiendler-Scharr, A., Nenes, A., and Weber, R. J.: Effectiveness of ammonia reduction on control of fine particle nitrate, *Atmos. Chem. Phys.*, 18, 12241-12256, 10.5194/acp-18-12241-2018, 2018.

Gwynn, R. C., Burnett, R. T., and Thurston, G. D.: A time-series analysis of acidic particulate matter and daily mortality and morbidity in the Buffalo, New York, region, *Environ Health Perspect*, 108, 125-133, 10.1289/ehp.00108125, 2000.

Hennigan, C. J., Izumi, J., Sullivan, A. P., Weber, R. J., and Nenes, A.: A critical evaluation of proxy methods used to estimate the acidity of atmospheric particles, *Atmos. Chem. Phys.*, 15, 2775-2790, 10.5194/acp-15-2775-2015, 2015.

Hu, J., Wang, Y., Ying, Q., and Zhang, H.: Spatial and temporal variability of PM<sub>2.5</sub> and PM<sub>10</sub> over the North China Plain and the Yangtze River Delta, China, *Atmospheric Environment*, 95, 598-609, <https://doi.org/10.1016/j.atmosenv.2014.07.019>, 2014.

Jang, M., Czoschke, N. M., Lee, S., and Kamens, R. M.: Heterogeneous Atmospheric Aerosol Production by Acid-Catalyzed Particle-Phase Reactions, *Science*, 298, 814, 10.1126/science.1075798, 2002.

Jia, S., Chen, W., Zhang, Q., Krishnan, P., Mao, J., Zhong, B., Huang, M., Fan, Q., Zhang, J., Chang, M., Yang, L., and Wang, X.: A quantitative analysis of the driving

factors affecting seasonal variation of aerosol pH in Guangzhou, China, *Science of The Total Environment*, 725, 138228, <https://doi.org/10.1016/j.scitotenv.2020.138228>, 2020.

Kim, K.-H., Kabir, E., and Kabir, S.: A review on the human health impact of airborne particulate matter, *Environment International*, 74, 136-143, <https://doi.org/10.1016/j.envint.2014.10.005>, 2015.

Kim, Y. P., and Seinfeld, J. H.: Atmospheric Gas–Aerosol Equilibrium: III. Thermodynamics of Crustal Elements Ca<sup>2+</sup>, K<sup>+</sup>, and Mg<sup>2+</sup>, *Aerosol Science and Technology*, 22, 93-110, 10.1080/02786829408959730, 1995.

Kleinman, M. T., Phalen, R. F., Mautz, W. J., Mannix, R. C., McClure, T. R., and Crocker, T. T.: Health effects of acid aerosols formed by atmospheric mixtures, *Environ Health Perspect*, 79, 137-145, 10.1289/ehp.8979137, 1989.

Kong, L., Tang, X., Zhu, J., Wang, Z., Pan, Y., Wu, H., Wu, L., Wu, Q., He, Y., Tian, S., Xie, Y., Liu, Z., Sui, W., Han, L., and Carmichael, G.: Improved Inversion of Monthly Ammonia Emissions in China Based on the Chinese Ammonia Monitoring Network and Ensemble Kalman Filter, *Environ Sci Technol*, 53, 12529-12538, 10.1021/acs.est.9b02701, 2019.

Lawal, A. S., Guan, X., Liu, C., Henneman, L. R. F., Vasilakos, P., Bhogineni, V., Weber, R. J., Nenes, A., and Russell, A. G.: Linked Response of Aerosol Acidity and Ammonia to SO<sub>2</sub> and NO<sub>x</sub> Emissions Reductions in the United States, *Environ Sci Technol*, 52, 9861-9873, 10.1021/acs.est.8b00711, 2018.

Li, J., and Jang, M.: Aerosol Acidity Measurement Using Colorimetry Coupled With a Reflectance UV-Visible Spectrometer, *Aerosol Science and Technology*, 46, 833-842, 10.1080/02786826.2012.669873, 2012.

Li, S., Ma, Z., Xiong, X., Christiani, D. C., Wang, Z., and Liu, Y.: Satellite and Ground Observations of Severe Air Pollution Episodes in the Winter of 2013 in Beijing, China, *Aerosol and Air Quality Research*, 16, 977-989, 10.4209/aaqr.2015.01.0057, 2016.

Liu, M., Song, Y., Zhou, T., Xu, Z., Yan, C., Zheng, M., Wu, Z., Hu, M., Wu, Y., and Zhu, T.: Fine particle pH during severe haze episodes in northern China, *Geophysical Research Letters*, 44, 5213-5221, 10.1002/2017GL073210, 2017.

Liu, P., Zhang, C., Mu, Y., Liu, C., Xue, C., Ye, C., Liu, J., Zhang, Y., and Zhang, H.: The possible contribution of the periodic emissions from farmers' activities in the North China Plain to atmospheric water-soluble ions in Beijing, *Atmos. Chem. Phys.*, 16, 10097-10109, 10.5194/acp-16-10097-2016, 2016.

Losey, D. J., Parker, R. G., and Freedman, M. A.: pH Dependence of Liquid–Liquid Phase Separation in Organic Aerosol, *The Journal of Physical Chemistry Letters*, 7, 3861-3865, 10.1021/acs.jpcllett.6b01621, 2016.

Losey, D. J., Ott, E.-J. E., and Freedman, M. A.: Effects of High Acidity on Phase Transitions of an Organic Aerosol, *The Journal of Physical Chemistry A*, 122, 3819-3828, 10.1021/acs.jpca.8b00399, 2018.

Lyu, B., Zhang, Y., and Hu, Y.: Improving PM<sub>2.5</sub> Air Quality Model Forecasts in China Using a Bias-Correction Framework, *Atmosphere*, 8, 10.3390/atmos8080147, 2017.

Mesinger, F., DiMego, G., Kalnay, E., Mitchell, K., Shafran, P. C., Ebisuzaki, W., Jović, D., Woollen, J., Rogers, E., Berbery, E. H., Ek, M. B., Fan, Y., Grumbine, R., Higgins, W., Li, H., Lin, Y., Manikin, G., Parrish, D., and Shi, W.: North American Regional Reanalysis, *Bulletin of the American Meteorological Society*, 87, 343-360, 10.1175/bams-87-3-343, 2006.

Mo, Y., Li, J., Liu, J., Zhong, G., Cheng, Z., Tian, C., Chen, Y., and Zhang, G.: The influence of solvent and pH on determination of the light absorption properties of water-soluble brown carbon, *Atmospheric Environment*, 161, 90-98, <https://doi.org/10.1016/j.atmosenv.2017.04.037>, 2017.

National Atmospheric Deposition Program: Ammonia Monitoring Network (AMoN), in, <http://nadp.slh.wisc.edu/AMoN/>.

Nenes, A., Pandis, S. N., Weber, R. J., and Russell, A.: Aerosol pH and liquid water content determine when particulate matter is sensitive to ammonia and nitrate availability, *Atmos. Chem. Phys.*, 20, 3249-3258, 10.5194/acp-20-3249-2020, 2020.

Oakes, M., Ingall, E. D., Lai, B., Shafer, M. M., Hays, M. D., Liu, Z. G., Russell, A. G., and Weber, R. J.: Iron Solubility Related to Particle Sulfur Content in Source Emission and Ambient Fine Particles, *Environ Sci Technol*, 46, 6637-6644, 10.1021/es300701c, 2012.

Pathak, R. K., Wu, W. S., and Wang, T.: Summertime PM<sub>2.5</sub> ionic species in four major cities of China: nitrate formation in an ammonia-deficient atmosphere, *Atmos. Chem. Phys.*, 9, 1711-1722, 10.5194/acp-9-1711-2009, 2009.

Pathak, R. K., Wang, T., Ho, K. F., and Lee, S. C.: Characteristics of summertime PM<sub>2.5</sub> organic and elemental carbon in four major Chinese cities: Implications of high acidity for water-soluble organic carbon (WSOC), *Atmospheric Environment*, 45, 318-325, <https://doi.org/10.1016/j.atmosenv.2010.10.021>, 2011.

Puchalski, M. A., Rogers, C. M., Baumgardner, R., Mishoe, K. P., Price, G., Smith, M. J., Watkins, N., and Lehmann, C. M.: A statistical comparison of active and passive ammonia measurements collected at Clean Air Status and Trends Network (CASTNET) sites, *Environmental Science: Processes & Impacts*, 17, 358-369, 10.1039/C4EM00531G, 2015.

Pye, H. O. T., Nenes, A., Alexander, B., Ault, A. P., Barth, M. C., Clegg, S. L., Collett Jr, J. L., Fahey, K. M., Hennigan, C. J., Herrmann, H., Kanakidou, M., Kelly, J. T., Ku, I. T., McNeill, V. F., Riemer, N., Schaefer, T., Shi, G., Tilgner, A., Walker, J. T., Wang, T.,

Weber, R., Xing, J., Zaveri, R. A., and Zuend, A.: The acidity of atmospheric particles and clouds, *Atmos. Chem. Phys.*, 20, 4809-4888, 10.5194/acp-20-4809-2020, 2020.

Seinfeld, J. H., and Pandis, S. N.: *Atmospheric chemistry and physics: from air pollution to climate change*, John Wiley & Sons, Inc., Hoboken, xxviii + 1203 pp. pp., 2006.

Shen, H. Z., Tao, S., Liu, J. F., Huang, Y., Chen, H., Li, W., Zhang, Y. Y., Chen, Y. C., Su, S., Lin, N., Xu, Y. Y., Li, B. G., Wang, X. L., and Liu, W. X.: Global lung cancer risk from PAH exposure highly depends on emission sources and individual susceptibility, *Scientific Reports*, 4, 10.1038/srep06561, 2014.

Shi, G., Xu, J., Peng, X., Xiao, Z., Chen, K., Tian, Y., Guan, X., Feng, Y., Yu, H., Nenes, A., and Russell, A. G.: pH of Aerosols in a Polluted Atmosphere: Source Contributions to Highly Acidic Aerosol, *Environ Sci Technol*, 51, 4289-4296, 10.1021/acs.est.6b05736, 2017.

Shi, X., Nenes, A., Xiao, Z., Song, S., Yu, H., Shi, G., Zhao, Q., Chen, K., Feng, Y., and Russell, A. G.: High-Resolution Data Sets Unravel the Effects of Sources and Meteorological Conditions on Nitrate and Its Gas-Particle Partitioning, *Environ Sci Technol*, 53, 3048-3057, 10.1021/acs.est.8b06524, 2019.

Sickles, I. J. E., Hodson, L. L., and Vorburger, L. M.: Evaluation of the filter pack for long-duration sampling of ambient air, *Atmospheric Environment*, 33, 2187-2202, [https://doi.org/10.1016/S1352-2310\(98\)00425-7](https://doi.org/10.1016/S1352-2310(98)00425-7), 1999.

Sickles, J. E., and Shadwick, D. S.: Comparison of particulate sulfate and nitrate at collocated CASTNET and IMPROVE sites in the eastern US, *Atmospheric Environment*, 42, 2062-2073, <https://doi.org/10.1016/j.atmosenv.2007.11.051>, 2008.

Song, S., Gao, M., Xu, W., Shao, J., Shi, G., Wang, S., Wang, Y., Sun, Y., and McElroy, M. B.: Fine-particle pH for Beijing winter haze as inferred from different thermodynamic equilibrium models, *Atmos. Chem. Phys.*, 18, 7423-7438, 10.5194/acp-18-7423-2018, 2018.

Song, S., Nenes, A., Gao, M., Zhang, Y., Liu, P., Shao, J., Ye, D., Xu, W., Lei, L., Sun, Y., Liu, B., Wang, S., and McElroy, M. B.: Thermodynamic Modeling Suggests Declines in Water Uptake and Acidity of Inorganic Aerosols in Beijing Winter Haze Events during 2014/2015–2018/2019, *Environmental Science & Technology Letters*, 6, 752-760, 10.1021/acs.estlett.9b00621, 2019.

Surratt, J. D., Chan, A. W. H., Eddingsaas, N. C., Chan, M., Loza, C. L., Kwan, A. J., Hersey, S. P., Flagan, R. C., Wennberg, P. O., and Seinfeld, J. H.: Reactive intermediates revealed in secondary organic aerosol formation from isoprene, *Proceedings of the National Academy of Sciences*, 107, 6640, 10.1073/pnas.0911114107, 2010.

Tao, Y., and Murphy, J. G.: The sensitivity of PM<sub>2.5</sub> acidity to meteorological parameters and chemical composition changes: 10-year records from six Canadian monitoring sites, *Atmos. Chem. Phys.*, 19, 9309-9320, 10.5194/acp-19-9309-2019, 2019.

Theobald, M. R., Simpson, D., and Vieno, M.: Improving the spatial resolution of air-quality modelling at a European scale—development and evaluation of the Air Quality Re-gridder Model (AQR v1. 1), *Geoscientific Model Development*, 9, 4475-4489, 2016.

Tian, S., Pan, Y., and Wang, Y.: Ion balance and acidity of size-segregated particles during haze episodes in urban Beijing, *Atmospheric Research*, 201, 159-167, <https://doi.org/10.1016/j.atmosres.2017.10.016>, 2018.

United States Environmental Protection Agency: Clean Air Status and Trends Network (CASTNET), in, <https://www.epa.gov/castnet>.

United States Environmental Protection Agency: CASTNET Quality Assurance Quarterly Report, United States Environmental Protection Agency, 2012a.

2011 National Emissions Inventory (NEI) Data: <https://www.epa.gov/air-emissions-inventories/2011-national-emissions-inventory-nei-data>, 2012b.

United States Environmental Protection Agency: CMAQ (Version 5.0.2) [Software], in, 2014.

Vasilakos, P., Russell, A., Weber, R., and Nenes, A.: Understanding nitrate formation in a world with less sulfate, *Atmos. Chem. Phys.*, 18, 12765-12775, 10.5194/acp-18-12765-2018, 2018.

Wang, G., Zhang, R., Gomez, M. E., Yang, L., Levy Zamora, M., Hu, M., Lin, Y., Peng, J., Guo, S., Meng, J., Li, J., Cheng, C., Hu, T., Ren, Y., Wang, Y., Gao, J., Cao, J., An, Z., Zhou, W., Li, G., Wang, J., Tian, P., Marrero-Ortiz, W., Secret, J., Du, Z., Zheng, J., Shang, D., Zeng, L., Shao, M., Wang, W., Huang, Y., Wang, Y., Zhu, Y., Li, Y., Hu, J., Pan, B., Cai, L., Cheng, Y., Ji, Y., Zhang, F., Rosenfeld, D., Liss, P. S., Duce, R. A., Kolb, C. E., and Molina, M. J.: Persistent sulfate formation from London Fog to Chinese haze, *Proceedings of the National Academy of Sciences*, 113, 13630-13635, 10.1073/pnas.1616540113, 2016.

Wang, R., Tao, S., Balkanski, Y., Ciais, P., Boucher, O., Liu, J., Piao, S., Shen, H., Vuolo, M. R., Valari, M., Chen, H., Chen, Y., Cozic, A., Huang, Y., Li, B., Li, W., Shen, G., Wang, B., and Zhang, Y.: Exposure to ambient black carbon derived from a unique inventory and high-resolution model, *Proceedings of the National Academy of Sciences*, 111, 2459-2463, 10.1073/pnas.1318763111, 2014a.

Wang, S., Wang, L., Li, Y., Wang, C., Wang, W., Yin, S., and Zhang, R.: Effect of ammonia on fine-particle pH in agricultural regions of China: comparison between urban and rural sites, *Atmos. Chem. Phys.*, 20, 2719-2734, 10.5194/acp-20-2719-2020, 2020a.

Wang, Y., Ying, Q., Hu, J., and Zhang, H.: Spatial and temporal variations of six criteria air pollutants in 31 provincial capital cities in China during 2013–2014, *Environment International*, 73, 413-422, <https://doi.org/10.1016/j.envint.2014.08.016>, 2014b.

Wang, Y., Gong, Z., Liu, Z. L., Tang, G., Cheng, L., Che, F., Gao, J., and Ji, D.: Construction and Application of Comprehensive Observation Network for Air

Pollution in Beijing-Tianjin-Hebei and Its Surrounding Areas(In Chinese), *Environmental Science Research*, 32, 1651-1663, 10.13198/j.issn.1001-6929.2019.09.12, 2019.

Wang, Y., Chen, Y., Wu, Z., Shang, D., Bian, Y., Du, Z., Schmitt, S. H., Su, R., Gkatzelis, G. I., Schlag, P., Hohaus, T., Voliotis, A., Lu, K., Zeng, L., Zhao, C., Alfarra, M. R., McFiggans, G., Wiedensohler, A., Kiendler-Scharr, A., Zhang, Y., and Hu, M.: Mutual promotion between aerosol particle liquid water and particulate nitrate enhancement leads to severe nitrate-dominated particulate matter pollution and low visibility, *Atmos. Chem. Phys.*, 20, 2161-2175, 10.5194/acp-20-2161-2020, 2020b.

Weber, R. J., Guo, H. Y., Russell, A. G., and Nenes, A.: High aerosol acidity despite declining atmospheric sulfate concentrations over the past 15 years, *Nat Geosci*, 9, 282-+, 10.1038/Ngeo2665, 2016.

William C. Skamarock , J. B. K., Jimmy Dudhia , David O. Gill , Dale M. Barker , Wei Wang , Jordan G. Powers: A description of the Advanced Research WRF version 3. NCAR Technical note -475+STR, 2008.

Xie, Y., Wang, G., Wang, X., Chen, J., Chen, Y., Tang, G., Wang, L., Ge, S., Xue, G., Wang, Y., and Gao, J.: Observation of nitrate dominant PM<sub>2.5</sub> and particle pH elevation in urban Beijing during the winter of 2017, *Atmos. Chem. Phys. Discuss.*, 2019, 1-25, 10.5194/acp-2019-541, 2019.

Yao, X., Chan, C. K., Fang, M., Cadle, S., Chan, T., Mulawa, P., He, K., and Ye, B.: The water-soluble ionic composition of PM<sub>2.5</sub> in Shanghai and Beijing, China, *Atmospheric Environment*, 36, 4223-4234, [https://doi.org/10.1016/S1352-2310\(02\)00342-4](https://doi.org/10.1016/S1352-2310(02)00342-4), 2002.

Yarwood, G., Rao, S., Yocke, M. A., and Whitten, G. Z.: Updates to the Carbon Bond Chemical Mechanism: CB05, 2005.

Ye, D., Klein, M., Mulholland, J. A., Russell, A. G., Weber, R., Edgerton, E. S., Chang, H. H., Sarnat, J. A., Tolbert, P. E., and Ebel Sarnat, S.: Estimating Acute Cardiovascular Effects of Ambient PM(2.5) Metals, *Environ Health Perspect*, 126, 027007, 10.1289/ehp2182, 2018.

Zhang, Q., Zheng, Y., Tong, D., Shao, M., Wang, S., Zhang, Y., Xu, X., Wang, J., He, H., Liu, W., Ding, Y., Lei, Y., Li, J., Wang, Z., Zhang, X., Wang, Y., Cheng, J., Liu, Y., Shi, Q., Yan, L., Geng, G., Hong, C., Li, M., Liu, F., Zheng, B., Cao, J., Ding, A., Gao, J., Fu, Q., Huo, J., Liu, B., Liu, Z., Yang, F., He, K., and Hao, J.: Drivers of improved PM<sub>2.5</sub>; air quality in China from 2013 to 2017, *Proceedings of the National Academy of Sciences*, 116, 24463, 10.1073/pnas.1907956116, 2019.

Zhang, R., Jing, J., Tao, J., Hsu, S. C., Wang, G., Cao, J., Lee, C. S. L., Zhu, L., Chen, Z., Zhao, Y., and Shen, Z.: Chemical characterization and source apportionment of

PM<sub>2.5</sub> in Beijing: seasonal perspective, *Atmos. Chem. Phys.*, 13, 7053-7074, 10.5194/acp-13-7053-2013, 2013.

Zhao, M., Wang, S., Tan, J., Hua, Y., Wu, D., and Hao, J.: Variation of Urban Atmospheric Ammonia Pollution and its Relation with PM<sub>2.5</sub> Chemical Property in Winter of Beijing, China, *Aerosol and Air Quality Research*, 16, 1390-1402, 10.4209/aaqr.2015.12.0699, 2016.

Zheng, G., Su, H., Wang, S., Andreae, M. O., Pöschl, U., and Cheng, Y.: Multiphase buffer theory explains contrasts in atmospheric aerosol acidity, *Science*, 369, 1374, 10.1126/science.aba3719, 2020.

Zheng, G. J., Duan, F. K., Su, H., Ma, Y. L., Cheng, Y., Zheng, B., Zhang, Q., Huang, T., Kimoto, T., Chang, D., Pöschl, U., Cheng, Y. F., and He, K. B.: Exploring the severe winter haze in Beijing: the impact of synoptic weather, regional transport and heterogeneous reactions, *Atmos. Chem. Phys.*, 15, 2969-2983, 10.5194/acp-15-2969-2015, 2015.